Swinging up and Stabilization of Cart Inverted Pendulum System Using Backstepping State Feedback Control Incorporating with GA

Tsiyon Nigusse Beyene

A Thesis Submitted to

The Department of Electrical Power and Control Engineering

School of Electrical Engineering and Computing

Presented in Partial Fulfilment of the Requirement for the Master of Science Degree in Electrical Power and Control Engineering (Specialization in Control Engineering)

Office of Graduate Studies

Adama Science and Technology University

November 2022

Adama, Ethiopia

Swinging up and Stabilization of Cart Inverted Pendulum System Using Backstepping State Feedback Control of Incorporating with GA

Tsiyon Nigusse Beyene

Advisor: Prof. Gang Gyoo Jin

Co-Advisor: Endriyas Alemayehu (MSc)

A Thesis Submitted to

The Department of Electrical Power and Control Engineering

School of Electrical Engineering and Computing

Presented in Partial Fulfillment of the Requirement for the Master of Science Degree in Electrical Power and Control Engineering (Specialization in Control Engineering)

Office of Graduate Studies

Adama Science and Technology University

November 2022

Adama, Ethiopia

DECLARATION

I hereby declare that this Master's Thesis entitled "Swinging up and Stabilization of Cart Inverted Pendulum System Using Backstepping State Feedback Control of Incorporating with GA" is my original work. That is, it has not been submitted for the award of any academic degree, diploma, or certificate in any other university. All sources of materials used in this thesis have been properly acknowledged through citation.

Tsiyon Nigusse Beyene		11/14/2022
Name of student	Signature	Date

RECOMMENDATION

We, the advisors of this thesis, hereby certify that we have read the revised version of the thesis entitled “Swinging up and Stabilization of Cart Inverted Pendulum System Using Backstepping State Feedback Control of Incorporating with GA” prepared under our guidance by Tsiyon Nigusse Beyene submitted in partial fulfilment of the requirements for the degree of Masters of Science in electrical power and control engineering (control). Therefore, we recommend the submission of the revised version of the thesis to the department following the applicable procedures.

Prof. Gang Gyoo Jin		11/14/2022
Major Advisor	Signature	Date

Endriyas Alemayehu (MSc.)		11/14/2022
Co-advisor	Signature	Date

APPROVAL SHEET

We, the advisors of this thesis entitled "Swinging up and Stabilization of Cart Inverted Pendulum System Using Backstepping State Feedback Control of Incorporating with GA" and developed by Tsiyon Nigusse Beyene, hereby certify that the recommendation and suggestions made by the board of examiners are appropriately incorporated into the final version of the thesis.

Prof. Gang Gyoo Jin		11/14/2022
Major Advisor	Signature	Date
		11/14/2022
Co-advisor	Signature	Date

We, the undersigned, members of the Board of Examiners of the thesis by Tsiyon Nigussie Beyene have read and evaluated the thesis entitled "Swinging up and Stabilization of Cart Inverted Pendulum System Using Backstepping State Feedback Control of Incorporating with GA" and examined the candidate during the open defence. This is, therefore, to certify that the thesis is accepted for partial fulfilment of the requirement of the degree of Master of Science in Control Engineering.

Chairperson	Signature	Date
Internal Examiner	Signature	Date
Dr. Chala Merga		09.Nov.2022
External Examiner	Signature	Date

Finally, approval and acceptance of the thesis are contingent upon the submission of its final copy to the Office of Postgraduate Studies (OPGS) through the Department Graduate Council (DGC) and School Graduate Committee (SGC).

Department Head	Signature	Date
School Dean	Signature	Date
Office of Postgraduate Studies, Dean	Signature	Date

ACKNOWLEDGMENT

First and foremost, I want to offer my whole-heartedly gratitude to Almighty **GOD**, his Mother **St. Mary** and all saints who guard me, for giving me the courage, patience and blessing to finish my graduate studies. I am extremely grateful to my advisor **Professor Gang Gyoo Jin**, for his insight guidance, support and encouragement on this work and give me a way how to deal with it to complete my thesis from his precious time due to his often-high workload. I am also really appreciative to my co-advisor **Mr. Endriyas Alemayehu (MSc.)** for his lots of advice and encouragement. My special thanks go to all instructors who thought me during my graduate study. No words of thanks are enough for my family for their unwavering devotion offered throughout the thesis work and graduate study. Last but not least, I am grateful to all of my colleagues for their support.

DEDICATION

To my father Nigussie Beyene, my mother Zewudinesh Mengesha, my sisters Betelihem Nigussie, Rediet Nigussie and Meron Nigussie.

Table of Contents

LIST OF TABLES

LIST OF FIGURES

LIST OF ABBREVIATIONS

BSF	Backstepping state feedback control
LQR	Linear quadratic regulating controller
IFAC	International Federation of Automatic Control
SIMO	Single input multi output
CIP	Cart inverted pendulum
FBD	Free Body Diagram
GA	Genetic Algorithm
IAE	Integral Absolute Error
MSP	Multiple set point change
IAU	Integral Absolute Error and control unit
MATLAB	Matrix Laboratory
SMC	Sliding Mode Control
UMS	Underactuated Mechanical Systems

ABSTRACT

The cart inverted pendulum system is an Underactuated system with one control input for two outputs degrees of freedom (DOF), highly nonlinear and inherently unstable. The pendulum is swinging from the pendant position to an inverted position when the cart is accelerated by force which is provided to the cart with a DC motor. In this thesis mathematical modelling of dynamics is derived by utilizing Euler-Lagrange's equations and the system is decomposed into cart subsystem and pendulum subsystem. Since the system is highly nonlinear, it can validate different nonlinear and linear controllers. So, in this work, a combined backstepping and state feedback controller is optimized by a genetic algorithm (GA) is designed for the stabilization of the system in a comparison with linear quadratic regulator (LQR) and energy-based passivity swing up a controller for swinging the pendulum from the pendant position to near to upright position. Additionally, there are four scenarios considered for the cart's position ± 1 *meter and* ± 45 *degrees the angle of a pendulum for proposed control effectivity. From the results in the simulation, the proposed controller gives 2.53% overshoot, 1.1695 settling time for set point changes responses and 63.26% of overshoot, 49.5474 IAE for multiple set point changes. For disturbance rejection, the proposed controller* $\pm$ *5N rejects disturbance applied at 2.0507 recovery time and 8.75519 IAE and robust to 40% change mass of pendulum to parameter uncertainty with 1.3106 and 1.8535 IAEU and IAE respectively. The performance of the controllers tuned with the genetic algorithm is measured using integral absolute error (IAE). The controller design is implemented in MATLAB.*

Keywords: *Backstepping, state feedback control, LQR, Cart inverted pendulum, Nonlinear system, GA Tuning*

CHAPTER ONE

INTRODUCTION

1.1 Background of the Study

Underactuated systems is a very interesting field of recent research as it is well presented and classified by (Olfati-saber, 2002). These systems have fewer actuators than the number of degrees of freedom, which makes control design more difficult, but it is also an interesting way to reduce costs and/or plan an emergency strategy in the event of a malfunction, leading to an underactuated behaviour.

The cart inverted pendulum system is a great example of an under-actuated, non-minimum phase, and highly unstable system (Coşkun, 2020). It has been used for many years as an effective test system for control theory. Because they exhibit nonlinear, unstable, non-minimum phase dynamics, and control objectives are always challenging (Y. Wang, n.d.). An inverted pendulum can be explained simply by comparing it to the childhood experiment of trying to balance a long stick on one finger. At first, they were used to illustrate linear control ideas such as stabilising unstable systems. Inverted pendulums have been useful due to their nonlinear nature, they are now used to illustrate many of the ideas emerging in the field of nonlinear control.

To compare new and existing control methods and tools in a meaningful way, the International Federation of Automatic Control (IFAC) Theory Committee came up with a collection of practical design issues in 1990. The committee developed a list of actual issues that were used as "benchmark control issues". Out of which the cascade inverted pendulum control problem is featured as highly unstable, and the toughness increases with increased links. The Inverted Pendulum is a single input multi output (SIMO) system with control voltage as input, cart position and pendulum angle as outputs (Kumar et al., 2013).

The research done on inverted pendulum control systems has a wide range of applications, including robot control technology like self-balancing robots (Son et al., 2014), attitude control of satellite flight (Finoki et al., 2015), tank missile launchers, design of earthquake-resistant buildings (Housner, 1963), vertical control in rocket launchers, stabilization of ships, Some two-wheeled personal conveyances with more manoeuvrability are created using inverted pendulum models and common industrial uses. Therefore, the inverted pendulum is widely used to evaluate new control strategies for this reason used frequently.

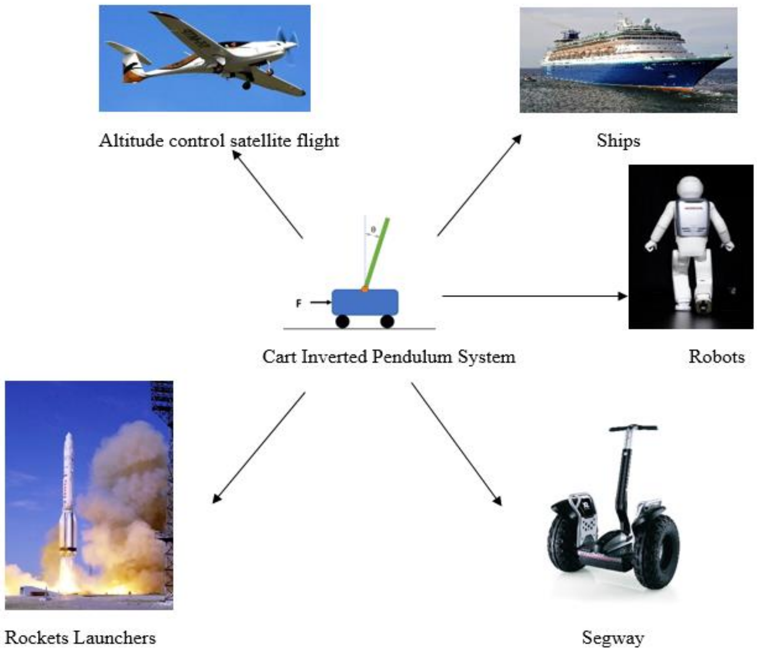

Figure 1.1 Some real applications of inverted pendulums

Underactuated mechanical systems appear in a variety of real-life control applications including Robotics. An inverted pendulum is significant for modelling in robotics control system design. Because it has redundancy, uncertainty, high coupling, and the natural characteristics of instability designing an appropriate control scheme for a nonlinear system becomes challenging. Zero dynamics of a system describe the internal behaviour when the output is kept at zero. Aside from the underactuated nature of the dynamics, the control problem is complex by the desire to stabilize the pendulum at an unstable equilibrium point (Ozbek & Efe,2010).

The system design is composed of three main subsystems: a mechanical system, a feedback network, and a control. This condition is the most basic when a pendulum is mounted on a cart that can move back and forth in a continuous linear direction basic. The pendulum is then brought into upright balance by managing the cart's movement. The theory of these controllers based on an approximate linear model can control the inverted pendulum system stability. The guiding principles to simplify the controller design for inverted pendulum systems lack in-depth discussion.

A critical review of an early history of nonlinear control shows that concepts related to optimality, stability, and uncertainty were descriptive rather than constructive. Scientific modelling of dynamical systems with state-space models and effective control designs for the system models are important in the control design of large and complex systems. In the design of any control problem, there are almost always inconsistencies between the actual plant and the mathematical model developed for controller design. This mismatch could be caused by unmodeled dynamics, changes in system parameters, or a simple model approximation of complicated plant behaviour. This provides a tool for analysing the stability of nonlinear systems (Ebrahim & Murphy,2005).

Backstepping has received a lot of attention in adaptive nonlinear control. Another energy-based technique is known as backstepping control. Backstepping allows for the preservation of relevant nonlinearities, which typically aid in the retention of finite values of the state vector without the need for linearization. This ensures that for a scalar system, a control law and Lyapunov control function that stabilizes its origin can be found. Lyapunov theory takes an important role in controller design and system convergence analysis and also provides an efficient tool for nonlinear systems of any order to build the control law and function of Lyapunov, which is the loop's stability, recursively, systematically, and directly.

Despite the widespread applicability of the scheme, the fact that it requires linearized plant dynamics is a drawback that renders the controller ineffective for operating points that differ from those utilized for linearization. So, combining the backstepping controller with the state feedback controller is done in this thesis for the nonlinear controller and also energy-based passivity swing-up control is used with stabilizing controller to get an effective and efficient result.

The cart-inverted pendulum system is one of the classical experimental systems that completely converge the complicated features of nonlinear control issues (Christensen & Christiansen, 2017). Accordingly, it’s important to design a controller that is used to stabilize, bring good performance, and weaken interference to the system to find out its effectiveness for the system. Backstepping state feedback controller to stabilize and energy passivity based control for swinging up is used in this study to improve the robustness of the cart inverted pendulum system. These control methods are designed and analysed in MATLAB simulation to illustrate an effective control system.

1.2 Statement of the problem

To balance the inverted pendulum on a cart that is rotating about the hinge to its upright position by swinging up the pendulum from its stable position to its inverted position under disturbance and parameter uncertainties is the main challenging issue of the system. Since the cart, inverted pendulum system is used as a test bed for robotic technology and many other real-time applications the stabilization and swinging-up control are the basic ones. Many controllers are developed for this system, from linear controllers to recent controllers like backstepping. In this thesis, the angular position of the pendulum is controlled by a nonlinear backstepping controller, and the cart position is controlled by a linear state feedback controller. This thesis investigates the combined backstepping state feedback controller as a solution for the stability problem of a cart inverted pendulum system in its upright (inverted) position under various scenarios. The swing up of the inverted pendulum from its downward position to its pendant position is solved by energy control using a passivity controller. GA optimization techniques are used to obtain optimal values.

1.3 Objectives of Study

1.3.1 General Objective

Studying the model, designing and analysing of backstepping state feedback stabilizing controller and energy based using passivity of pendulum swing up a controller for cart inverted pendulum system using GA optimization is the main objective of the thesis.

1.3.2 Specific Objective

- To study the mathematical model of the cart inverted pendulum system
- To design a combined backstepping state feedback controller.
- To design energy-based passivity of the pendulum swing-up controller.
- To evaluate and analyse the performance of the controller tuning with GA using MATLAB.

1.4 Significance of the Thesis

Nowadays, underactuated mechanical systems are becoming a hot issue in controlling nonlinear systems, these have an experimental testing ground that is an inverted pendulum cart. It is also important in modelling robotics control system design because of its redundancy, uncertainties and natural characteristics of instability. So, this study has a great role in the area of stabilization under different scenarios, parameter uncertainties and disturbance rejection on the various application used for present and future days. For this system, 40% of pendulum mass uncertainty and ± 5N disturbance is supported in the application used.

1.5 Scope of the Study

The thesis focuses on the mathematical model of a cart inverted pendulum and its electrical actuator, which swings the pendulum. Then, using GA optimization, design and test of backstepping state feedback stabilizing controller and an energy-based passivity of pendulum swing-up controller for the cart inverted pendulum.

1.6 Organization of the Thesis

This thesis has been organized into six chapters.

Chapter One: presents the background of the study, the statement of problems, the general and specific objectives of the study, significance and scope of the thesis.

Chapter Two: discuss the historical and theoretical background and related works on the control systems of cart inverted pendulum systems.

Chapter Three: described the mathematical modelling of the system, linearization of the nonlinear model and state space equation of the system.

Chapter Four: illustrates stabilization and swinging up controller design. Backstepping, state feedback, LQR, Energy-based passivity swing-up control and genetic algorithm optimization techniques are developed for the system.

Chapter Five: presents the simulation results, and the response to performance tests.

Chapter Six: Finally, discussions of the conclusion and recommendation.

CHAPTER TWO

THEORETICAL BACKGROUND AND LITERATURE REVIEW

Control systems can be found all around us, in nature, everyday life, and industry. Since most systems are inherently nonlinear, those problems are of interest to engineers, mathematicians, and many other scientists. The cart inverted pendulum represents a class of real-world systems, which adds to the interest and significance of the subject. The Cart-Pendulum System has been extensively researched to gain insight into the control algorithms developed for similar higher-order systems such as flexible link robots, flexible joint robots, space robots, mobile robots, rocket guidance systems, and underwater vehicles.

Control engineers have long attempted to solve this problem using various approaches. The first approach involved developing linear controllers such as PID (Lim et al., 2018), LQR (Kalyoncu, 2016) and other controllers based on linear models developed for systems that had various assumptions. Later, advances in the field of control systems led to the development of nonlinear control theories such as feedback linearization, (Fossen, 2019) sliding mode control,(Chaudhary, 2018; Kurode et al., 2011; Park & Chwa, 2009) back-stepping (Khudhair et al., 2021; Lee et al., 2017), adaptive control, passivity-based control (Jörgl et al., 2013), intelligent controllers based on genetic algorithms (Yusuf, n.d.), fuzzy logic (Muškinja & Tovornik, 2006), neural networks, particle swarm optimization, (Shima & Bashir, 2021) are most recently contracting system theory. The design of the nonlinear control law for the nonlinear control is the most complex, but it is also the most robust (Fernando et.al., 2015).

The cart inverted pendulum is an interesting and challenging problem due to its unique characteristics listed below:

- It is a nonlinear system
- It is unstable in the inverted position
- It is a non-minimum phase and zero dynamics system
- It is an underactuated system
- It is a SIMO system
- It is extensively sensitive to external disturbance

2.1 History of cart inverted pendulum systems

According to the author (Lundberg et al., 1986)**,** the cart inverted pendulum history starts with Roberge (1960) at M.I.T, in his aptly named bachelor's thesis, "The Mechanical Seal". He presented a solution to the inverted pendulum system. Leonard Gould supervises the research done by Roberge. Higdon and Cannon (1963) at Stanford University described systems with multiple independent inverted pendula. The multiple inverted pendulum mechanical system was proposed by Claude Shannon, the father of information theory and an enthusiastic unicyclist, according to a prominent footnote in Higdon's article that acknowledges Roberge's work. M.I.T Professor Claude Shannon recommended this model to the second author. (Experiments with a single pendulum are described in an SB thesis entitled "The Mechanical Seal" by Roberge at MIT, May 1960), (Lundberg et al., 1986)**.**
Inverted-pendulum systems with joints and flexibility were covered by Schaefer and Cannon in 1966. The system was also credited to Shannon in this article (which also shares a co-author with Higdon and Cannon (1963)), but Roberge's work is not mentioned. The dual-inverted-pendulum system was used as an illustration by Truxal (1965) in a set of lecture notes on state-space models and control. By the end of the 1960s, well-known textbooks like Cannon (1967), Dorf (1967), and Ogata (1970), all of reference to Higdon and Cannon (1963), also included the single inverted-pendulum method.

The stabilization of an inverted pendulum by a vertically swinging base is a common example in physics and classical mechanics presentations. In a series of articles published in the American Journal of Physics in 1965, Phelps & Hunter, Blitzer, and Kalmus explored this example system (1970). Inverted-pendulum system swing-up control was developed by Mori et al. in 1976 (referencing Schaefer and Cannon (1966) but nothing earlier). The rotational pendulum system was suggested by Furuta et al. as an alternative to the cart-on-track system (1991).

2.2 Review of Previous Works

There are a lot of papers done on reviewing controllers used on cart inverted pendulums. The authors (Krafes et al., 2016) and (H. Wang, 2011) review linear, nonlinear and intelligent controllers for inverted pendulums. The inverted pendulum has several invention based on its operating points. As it is done in many papers the main goal of the control law is to stabilize the pendulum around its upright position on unstable equilibrium points. In the paper (Krafes et al., 2016) reviewed different controllers such as LQR, PID, fuzzy logic, ANFIS, SMC, and backstepping controllers are reviewed.

In the paper (Coşkun, 2020) nonlinear sliding mode control and feedback linearization control are derived. But the author uses the linearized model of the dynamics of a cart inverted pendulum system around an unstable upright position and additionally the corresponding analysis uses the standard linear stability arguments and the traditional Lyapunov method. The proposed control law in the paper performs stabilization of initial conditions and reference tracking. The drawback of using SMC has a chattering problem that excites undesired flexible dynamics that cause system instability but the paper uses saturation function to mitigate along with it and also feedback linearization causes the system to behave contrarily to the original system due to its loss of non-linear response.

In the paper (Mansoor & Bhutta, 2016) genetic algorithm-based optimal backstepping (Fu & Lin, 2005) controller design for stabilizing an inverted pendulum is presented. A new fitness function based on the integral of the first derivative of output is used as performance criteria. Backstepping is done using Krasavoskii LaSalle Principle based on the Lyapunov function. But in this paper, the control signal used to stabilize the system doesn't contain the position of the angle. Although the author adds simply linear terms of the position of the angle and its derivative angular velocity of it to come up with four states of the system.

The authors (Tai et al., 2020) used a backstepping controller for the stabilization of a rotary inverted pendulum. To design the controller the paper first linearizes the dynamical model of a system. So, it applies a linear backstepping controller and also it compares two controllers for swing-up control, these are classical energy-based control and exponentiation of the pendulum position method. The control law derived is the output signal is a sine wave because the backstepping controller guarantees the first regulator to converge to zero. As the first regulator is a combination of the angle of the pendulum and the angle of the arm so, it doesn’t guarantee the angle of the pendulum and arm to move to zero. Therefore, these variables can still vibrate. However, due to the stability of the first regulator, these variables tend to be unstable. The paper shows a comparison using both the simulation and experimental results of swing up by energy-based control and swing up by exponentiation pendulum position method with stabilization using backstepping. Both swing-up by exponentiation pendulum position method with stabilization using the linear backstepping method shows better results.

The paper (Khati, 2020) focuses on the dynamic model of the robot manipulator by applying a backstepping controller based on the Lyapunov function for performing certain desired trajectories. Indeed, the majority of robot-interested jobs are delicate and demand extremely high precision while moving at rapid speeds. Advanced such resulted in the development of novel control techniques for robot manipulators. The paper carried a geometric, kinematic and dynamic model of a robot manipulator used in practical movement in space. Backstepping helps keep useful nonlinearities and also performs robustness in parametric variation up to 40 per cent for the robot joint masses. The drawback of the paper is it didn't compare the proposed controller with other linear or nonlinear controllers, because it helps how the proposed controller performs effectively.

The author (Patra et al., 2019) in this paper's novel controller is a Backstepping Linear Quadratic Gaussian controller design for balancing an inverted pendulum is presented. The paper analyses comparatively with optimal PID control, LQG and other robust controllers listed and presented by other authors in this paper many controllers are listed and show that they are not free from dependency on optimal settling of parameters and also these controllers are not completely insensitive to model uncertainties and disturbance. Hybrid controllers are proved in many cases a fruitful approach by mutual influence to compensate for individual limitations and provide a robust control technique. The proposed control law is formulated by modifying the linear quadratic regulator through a state estimator based on the backstepping control technique two steps are followed the first one is backstepping design for cart position and angle position θ the second one is the whole system is accordingly segregated into subsystem cascading approach is taken for both LQR with Kalman filter and backstepping control to design a novel control approach BLQG controller.

In this thesis, the backstepping controller is combined with the state feedback controller for the stabilization problem of the cart inverted pendulum system. During the literature review, many papers are done by the linearizing system around operating points which makes to be less effective in a wider basin of the system. So, designing a controller using hybrid control is a useful and effective approach since both provide important benefits and more robust control. For swing-up control also energy based with passivity control is combined and when it approaches the upright position backstepping state feedback control takes over and quickly the system becomes stabilized. In general, the proposed controller technique shows better performance in all aspects compared to the LQR controller.

CHAPTER THREE

MATHEMATICAL MODEL OF CART INVERTED PENDULUM

This chapter deals with obtaining the mathematical model of a cart inverted pendulum. The main goal is to find the equations that describe the motion of the system in a state space form. Then linearization of the nonlinear system around operating points for the help of designing linear control.

3.1. Parameters and Their Symbols Needed for Modelling

This inverted pendulum system is an instance system for real-time applications found in many types of research. The interesting aspect of this mechanism is that it is unstable while uncontrolled, this is, and the pendulum is going to simply fall over if the cart isn't moved to balance it. Also, the system is non-linear. The control system's goal is to balance the inverted pendulum by exerting force on the cart to which the pendulum is attached. In such a case, as indicated in Figure 3.1, it is shown a two-dimensional pendulum issue at the ground plane and the free body diagram helps to illustrate each structure. The force F that drives the cart horizontally acts as the system's control input, and its outputs are the angular position of the pendulum θ and the horizontal position of the cart x.

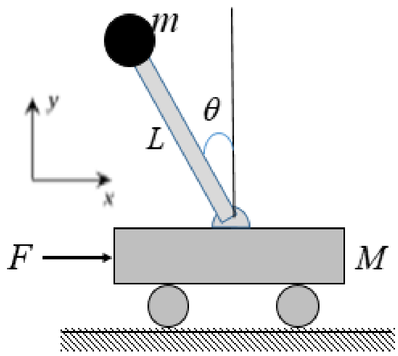

Figure 3. 1 FBD diagram of cart inverted pendulum

Table 3.1 Parameter of a cart inverted pendulum system

Parameters	Description	Values	Unit
M	Mass of cart	0.94	Kg
m	Mass of pendulum	0.23	Kg
J	Moment of inertia of the pendulum	0.000788	$Kg.m^2$
x	Position of cart	-	m
θ	Angle of pendulum	-	rad
x_{pend}	Vertical displacement of the pendulum	-	m
x_{cart}	Horizontal displacement of cart	-	m
L	Length from hinge point to pendulum centre of gravity	0.3302	m
g	Acceleration due to gravity	9.81	m/s^2
b_{eq}	Coefficient of cart friction	5.4	$N.s/m$
b_p	Viscous damping friction of pendulum	0.0024	$N.s.m/rad$
F	Driving force of the cart	-	N
KE	Kinetic Energy	-	J
PE	Potential Energy	-	J

The cart inverted pendulum is single input multiple outputs (SIMO Underactuated system). It has one input and two outputs. The system may seem simple but modelling and controlling is a challenging task.

- The electrical subsystem creates the desired force according to a reference.
- The mechanical subsystem that receives this force

3.2 Modelling Mechanical Part of the System

The mathematical model of the cart inverted pendulum problem is derived by using either Newtonian or Lagrangian approaches. It has been verified that the equation coming from both approaches is the same and hence warrants the validity of the derived mathematical model, (Kumar et al., 2013). So, this thesis Euler-Lagrangian equation has been chosen to do the modelling approach used for the cart inverted pendulum system. The Lagrangian of a system is the difference between the kinetic energy and potential energy of the system. It is assumed that the vertical force has no impact on the cart positions and that the horizontal movement is controlled by the force via the operation of the DC motor.

a) Kinematic equations

The first thing to consider for the system is kinematic equations

$$X_{cart,i} = x, X_{cart,j} = 0;$$

$$X_{pend,i} = x + l\sin\theta, X_{pend,j} = l\cos\theta;$$

$$\therefore\ X_0 = \begin{bmatrix} 0 \\ 0 \end{bmatrix}, X_{cart} = \begin{bmatrix} x \\ 0 \end{bmatrix}, X_{pend} = \begin{bmatrix} x + l\sin\theta \\ l\cos\theta \end{bmatrix};$$

Where X_0 the origin of the system is, X_{cart} is the position vector of the cart, X_{pend} is the position vector of the pendulum.

To find the velocity of the cart and the angular velocity of the pendulum we have to derivate the position of the cart and the position (angle) of the pendulum,

$$\dot{X}_{cart} = \begin{bmatrix} \dot{x} \\ 0 \end{bmatrix}, \dot{X}_{pend} = \begin{bmatrix} \dot{x} + l\dot{\theta}\cos\theta \\ -l\dot{\theta}\sin\theta \end{bmatrix}; \text{ Let } q = \begin{bmatrix} x \\ \theta \end{bmatrix} \text{ then,}$$

The equations of motion are obtained using Lagrange Equations. Define that the Lagrangian function L is the difference between the system's kinetic and potential energy. The kinetic energy for the pendulum can be described with two components, the kinetic energy from the linear motion of the rod as a point mass at the pendulum centre of gravity, and the kinetic energy KE from the rotational motion around the hinge point, generated by the moment of inertia around the pendulum centre of gravity. The system's potential energy PE is made up of the combined potential energies of the cart and the rod.

Kinetic Energy of the system, $KE(q,\dot{q}) = \frac{1}{2}M\left|\dot{X}_{cart}\right|^2 + \frac{1}{2}m\left|\dot{X}_{pend}\right|^2 + \frac{1}{2}J\dot{\theta}^2$ (3.1)

$$\left|\dot{X}_{cart}\right|^2 = \dot{x}^2 + 0 = \dot{x}^2, \tag{3.2a}$$

$$\left|\dot{X}_{pend}\right|^2 = \left(\dot{x} + l\dot{\theta}\cos\theta\right)^2 + \left(-l\dot{\theta}\sin\theta\right)^2 = \dot{x}^2 + 2\dot{x}l\dot{\theta}\cos\theta + l^2\dot{\theta}^2\cos^2\theta + l^2\dot{\theta}^2\sin^2\theta$$
$$= \dot{x}^2 + 2\dot{x}l\dot{\theta}\cos\theta + l^2\dot{\theta}^2 \tag{3.2b}$$

Since, $\cos^2\theta + \sin^2\theta = 1$ trigonometric identity

$$\therefore KE(q,\dot{q}) = \frac{1}{2}\left(M+m\right)\dot{x}^2 + m\dot{x}l\dot{\theta}\cos\theta + \frac{1}{2}\left(J+ml^2\right)\dot{\theta}^2 \tag{3.3}$$

$$KE(q,\dot{q}) = \frac{1}{2}\begin{bmatrix}\dot{x} & \dot{\theta}\end{bmatrix}\begin{bmatrix} M+m & ml\cos\theta \\ ml\cos\theta & J+ml^2 \end{bmatrix}\begin{bmatrix}\dot{x} \\ \dot{\theta}\end{bmatrix} = \frac{1}{2}\dot{q}^T M(q)q \tag{3.4}$$

Where, $M(q) = \begin{bmatrix} M+m & ml\cos\theta \\ ml\cos\theta & J+ml^2 \end{bmatrix}$

The potential energy in the system is given by the gravitational force acting on the system components. Because the cart only can move in the horizontal direction, which is perpendicular to the gravitational force, the cart cannot have any change in potential energy.

Therefore the Potential Energy of the system,

$$PE(q) = PE_{cart}(q) + PE_{pend}(q) \tag{3.5}$$

$$PE(q) = mgX_{pend} + mgX_{cart}\text{, since } X_{cart} = 0 \text{ then,} \tag{3.6}$$

$$PE(q) = mgl\cos\theta \tag{3.7}$$

Equation (3.8) is defined only from the pendulum position since the cart moves only horizontally

$$\frac{d}{dt}\left(\frac{\partial L}{\partial \dot{q}}\right) - \left(\frac{\partial L}{\partial q}\right) = \tau \tag{3.8}$$

The Euler-Lagrangian equation of motion for a mechanical system is given by:

$$L = KE(q,\dot{q}) - PE(q) \tag{3.9}$$

Where L=Lagrangian of system, τ =Resultant Force/ Torque

$$\frac{\partial KE(q,\dot{q})}{\partial \dot{q}} = \frac{\partial}{\partial \dot{q}}\left(\frac{1}{2}\dot{q}^T M(q)\dot{q}\right) = \frac{1}{2}M(q)\dot{q} + \frac{1}{2}\dot{q}^T M(q) + \frac{1}{2}\dot{q}^T\left(\frac{\partial M(q)}{\partial q}\right) \tag{3.10}$$

But $\frac{\partial M(q)}{\partial q} = 0 \ \therefore \frac{\partial KE(q,\dot{q})}{\partial \dot{q}} = \frac{1}{2}M(q)\dot{q} + \frac{1}{2}M(q)^T\dot{q}$ (3.11)

But $M(q)^T = M(q)$ is a skew-symmetric matrix

$\therefore \frac{\partial KE(q,\dot{q})}{\partial \dot{q}} = M(q)\dot{q}$ And $\frac{\partial PE(q)}{\partial \dot{q}} = 0$ then $\therefore \frac{\partial L}{\partial \dot{q}} = M(q)\dot{q}$

$$\frac{d}{dt}\left(\frac{\partial L}{\partial \dot{q}}\right) = \frac{d}{dt}\left(M(q)\dot{q}\right) = \dot{M}(q)\dot{q} + M(q)\ddot{q} \tag{3.12}$$

$M(q) = \begin{bmatrix} M+m & ml\cos\theta \\ ml\cos\theta & J+ml^2 \end{bmatrix}$ And $\dot{M}(q) = \begin{bmatrix} 0 & -ml\dot{\theta}\sin\theta \\ -ml\dot{\theta}\sin\theta & 0 \end{bmatrix}$

In the cart pendulum system, the chosen coordinates are the cart (x) and the pendulum (θ) displacement, which leads to the following Euler-Lagrangian equation with the corresponding partial derivatives.

$$\frac{\partial L}{\partial q} = \frac{\partial KE(q,\dot{q})}{\partial q} - \frac{\partial PE(q)}{\partial q} \tag{3.13}$$

From Eqn. (3.3) and Eqn. (3.7) $\frac{\partial KE(q,\dot{q})}{\partial x} = 0, \frac{\partial KE(q,\dot{q})}{\partial \theta} = m\dot{x}\dot{\theta}l\sin\theta$

Since the Lagrangian function L does not depend on x, follows

$$\frac{\partial PE(q)}{\partial x} = 0, \frac{\partial PE(q)}{\partial \theta} = -mgl\sin\theta \tag{3.14}$$

$\frac{\partial KE(q,\dot{q})}{\partial q} = \begin{bmatrix} \frac{\partial KE(q,\dot{q})}{\partial x} \\ \frac{\partial KE(q,\dot{q})}{\partial \theta} \end{bmatrix} = \begin{bmatrix} 0 \\ m\dot{x}\dot{\theta}l\sin\theta \end{bmatrix}$ And $\frac{\partial PE(q)}{\partial q} = \begin{bmatrix} \frac{\partial PE(q)}{\partial x} \\ \frac{\partial PE(q)}{\partial \theta} \end{bmatrix} = \begin{bmatrix} 0 \\ -mgl\sin\theta \end{bmatrix}$

$$\therefore \frac{\partial L}{\partial q} = \begin{bmatrix} 0 \\ m\dot{x}\dot{\theta}l\sin\theta \end{bmatrix} - \begin{bmatrix} 0 \\ -mgl\sin\theta \end{bmatrix} = \begin{bmatrix} 0 & 0 \\ ml\dot{\theta}\sin\theta & 0 \end{bmatrix}\begin{bmatrix} \dot{x} \\ \theta \end{bmatrix} - \begin{bmatrix} 0 \\ -mgl\sin\theta \end{bmatrix} \tag{3.15}$$

$$\frac{\partial L}{\partial q} = \begin{bmatrix} 0 \\ ml\dot{\theta}\sin\theta \end{bmatrix}\dot{q} - \begin{bmatrix} 0 \\ -mgl\sin\theta \end{bmatrix}, \tag{3.16}$$

To collect each equation of kinetic and

$$L(x,\theta) = \frac{1}{2}\begin{bmatrix} \dot{x} \\ \dot{\theta} \end{bmatrix}^T \begin{bmatrix} M+m & ml\cos\theta \\ ml\cos\theta & J+ml^2 \end{bmatrix}\begin{bmatrix} \dot{x} \\ \dot{\theta} \end{bmatrix} - mgl\sin\theta \tag{3.17}$$

Where, $\tau = \begin{bmatrix} \tau_x \\ \tau_\theta \end{bmatrix} = \begin{bmatrix} \tau_c \\ \tau_p \end{bmatrix}$

τ_c = Resultant Force on Cart (F_R) =Applied force – Frictional force= $F - b_{eq}\dot{x}$ (3.18)

τ_p =Resultant Torque on Pendulum (F_R) =Applied Torque– Frictional torque= $0 - b_p\dot{\theta}$ (3.19)

Where F is the controlled applied force from the DC motor that moves the cart, as we know the cart inverted pendulum system has two degrees of freedom and F is the only force applied to the system that is capable of changing the cart's positon x and cart's velocity $\dot{x}$. However, no external force is applied to the system that affects θ it directly.

The Euler-Lagrangian equation for both cart and pendulum

$$\frac{d}{dt}\left(\frac{\partial L}{\partial \dot{x}}\right) - \frac{\partial L}{\partial x} = F - b_{eq}\dot{x} \tag{3.20a}$$

$$\frac{d}{dt}\left(\frac{\partial L}{\partial \theta}\right) - \frac{\partial L}{\partial \theta} = -b_p\dot{\theta} \tag{3.20b}$$

From the Euler-Lagrangian equation the state space representation of the cart-inverted pendulum system can be determined:

Adding Eqn. (3.12) and Eqn. (3.15) equating with Eqn. (3.20a) and Eqn. (3.20b) respectively;

$$\dot{M}(q)\begin{bmatrix} \dot{x} \\ \dot{\theta} \end{bmatrix} + M(q)\begin{bmatrix} \ddot{x} \\ \ddot{\theta} \end{bmatrix} - \begin{bmatrix} 0 & 0 \\ ml\dot{\theta}\sin\theta & 0 \end{bmatrix}\begin{bmatrix} \dot{x} \\ \dot{\theta} \end{bmatrix} - \begin{bmatrix} 0 \\ -mgl\sin\theta \end{bmatrix} = \begin{bmatrix} F - b_{eq}\dot{x} \\ -b_p\dot{\theta} \end{bmatrix} \tag{3.21}$$

From the above equation taking $\dot{M}(q)$ and $M(q)$

$$\begin{bmatrix} 0 & -ml\dot{\theta}\sin\theta \\ -ml\dot{\theta}\sin\theta & 0 \end{bmatrix}\begin{bmatrix} \dot{x} \\ \dot{\theta} \end{bmatrix} + \begin{bmatrix} M+m & ml\cos\theta \\ ml\cos\theta & J+ml^2 \end{bmatrix}\begin{bmatrix} \ddot{x} \\ \ddot{\theta} \end{bmatrix} + \begin{bmatrix} 0 & 0 \\ ml\dot{\theta}\sin\theta & 0 \end{bmatrix}\begin{bmatrix} \dot{x} \\ \dot{\theta} \end{bmatrix}$$

$$+\begin{bmatrix} 0 \\ -mgl\sin\theta \end{bmatrix} = \begin{bmatrix} F - b_{eq}\dot{x} \\ -b_p\dot{\theta} \end{bmatrix} \tag{3.22}$$

Collecting the same terms in Eqn. (3.22)

$$(M+m)\ddot{x} - ml\dot{\theta}^2\sin\theta + ml\cos\theta\ddot{\theta} = F - b_{eq}\dot{x} \tag{3.23a}$$

$$-ml\dot{\theta}\dot{x}\sin\theta + ml\cos\theta\ddot{x} + (J+ml^2)\ddot{\theta} + ml\dot{\theta}\dot{x}\sin\theta - mgl\sin\theta = -b_p\dot{\theta} \tag{3.23b}$$

3.3 State Space Representation of Nonlinear Cart Inverted Pendulum

Let $x_1 = x, x_2 = \dot{x}, x_3 = \theta, x_4 = \dot{\theta}$ and Force applied to the cart is input to the system $F = u$ having

$$\dot{x}_1 = x_2$$

$$\dot{x}_2 = \frac{(J+ml^2)mlx_4{}^2\sin x_3 - m^2l^2g\sin x_3\cos x_3 + ml\cos x_3 b_p x_4 - (J+ml^2)b_{eq}x_2 + (J+ml^2)u}{(J+ml^2)(M+m) - m^2l^2\cos^2 x_3}$$

$$\dot{x}_3 = x_4 \tag{3.24}$$

$$\dot{x}_4 = \frac{-m^2l^2x_4{}^2\sin x_3\cos x_3 + (M+m)mgl\sin x_3 + ml\cos x_3 b_{eq}x_2 - (M+m)b_p x_4 - ml\cos x_3 u}{(J+ml^2)(M+m) - m^2l^2\cos^2 x_3}$$

3.4 Linearization for a Nonlinear Model

Linearization is a technique for determining the local stability of an equilibrium point of nonlinear differential equations or a discrete dynamical system. Linearization allows techniques for analysing linear systems to be used to analyse the behaviour of a nonlinear system around a specified point of equilibrium.

Cart inverted pendulum has two equilibrium points or angles where the pendulum is downward position at an angle of $\theta = 180°$ and the second equilibrium point has an angle of $\theta = 0^0$ and is in the upright vertical position. Currently, the pendulum is balanced, but even the smallest perturbation will lead it to diverge from this equilibrium, oscillate, and eventually come to rest in the lowest position. It follows that to keep the pendulum in the upright position at the second equilibrium point, a constant control law must be applied.

Control strategy formulation for equilibrium is generally accepted as an initial attempt for any new control techniques as proof of further application in control system engineering. To investigate the nature of the system about its equilibrium points, such as its stability, poles, etc., a Jacobian linearization of the system about those points is necessary. In the vicinity of the operating/equilibrium point, Jacobian linearization utilizes the Taylor series expansion to approximate the nonlinear state space equations with linear ones. Let the linearized plant have the state space equation:

$$\Delta\dot{x} = A_m\Delta x + B_m\Delta u\,,\ \Delta y = C_m\Delta x + D_m\Delta u\,,\ \Delta x = x - x_{eq}\,,\ \Delta u = u - u_{eq} \tag{3.25}$$

x is state space defined in equation (3.24), u_{eq} is control action at equilibrium, x_{eq} is equilibrium value of states y_{eq} is output in equilibrium. Where A_m, B_m, C_m, and D_m are the linearized state space matrices. The x denotes the state variable, u denotes the control input, y and denotes the measured output. The state variable x comprised pendulum angular displacement θ cart position x pendulum angular velocity $\dot{\theta}$, and cart velocity $\dot{x}$.

Assume a small deviation θ from equilibrium, then $\cos\theta \approx 1, \sin\theta \approx \theta, \dot{\theta}^2 \approx 0$

In other words, $\cos\theta = \cos x_3 \approx 1, \sin\theta = \sin x_3 \approx \theta, \dot{\theta}^2 = {x_4}^2 \approx 0$

From the use of the above relationship and the following equation,

$$\begin{aligned}
\dot{x}_1 &= x_2 \\
\dot{x}_2 &= \frac{-m^2l^2gx_3 + mlb_px_4 - (J+ml^2)b_{eq}x_2 + (J+ml^2)u}{(J+ml^2)(M+m) - m^2l^2} \\
\dot{x}_3 &= x_4 \\
\dot{x}_4 &= \frac{(M+m)mglx_3 + mlb_{eq}x_2 - (M+m)b_px_4 - mlu}{(J+ml^2)(M+m) - m^2l^2}
\end{aligned} \tag{3.26}$$

$$D' = (J+ml^2)(M+m) - (ml)^2 \tag{3.27}$$

The linearized equation of the nonlinear system can be described in the state space form as

$$\begin{aligned} \dot{x} &= A_m x + B_m u \\ y &= C_m x + D_m u \end{aligned} \tag{3.28a}$$

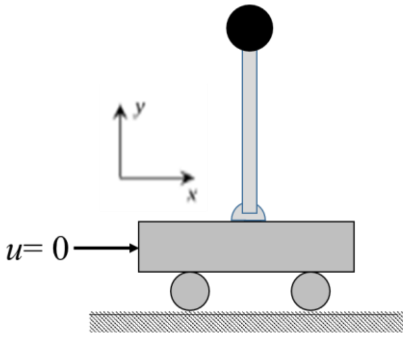

Figure 3. 2 Linearized model of cart inverted pendulum system

$$A_m = \begin{bmatrix} 0 & 1 & 0 & 0 \\ 0 & \dfrac{-(J+ml^2)b_{eq}}{D'} & \dfrac{-m^2l^2g}{D'} & \dfrac{mlb_p}{D'} \\ 0 & 0 & 0 & 1 \\ 0 & \dfrac{mlb_{eq}}{D'} & \dfrac{(M+m)mgl}{D'} & \dfrac{-(M+m)b_p}{D'} \end{bmatrix}, B_m = \begin{bmatrix} 0 \\ \dfrac{J+ml^2}{D'} \\ 0 \\ \dfrac{-ml}{D'} \end{bmatrix}$$

$$C_m = \begin{bmatrix} 1 & 0 & 0 & 0 \\ 0 & 0 & 1 & 0 \end{bmatrix} \tag{3.28b}$$

The system is linear and matrices A_m, B_m and C_m are time-invariant.

3.4 Mathematical Modelling of Electrical Subsystem

DC motor is used to generate a signal that actuates a cart that is used as the input signal to the system. By adjusting the motor's output torque angular position and the position of a cart can be changed. The speed of the DC motor can be controlled by varying the input DC voltage source. Armature control is the most common control technique for DC motors. These are two types: armature current control and armature voltage control. Armature voltage control and armature current control both need a source of controllable current and voltage that are proportional to the input control signal (Lemos, 2018).

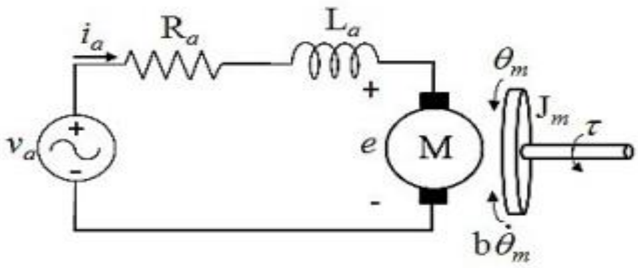

Figure 3. 3 Modelling of DC motor

The parameters of DC motor and its values are listed in the table below.

Table 3.2 Parameters of DC Motor

Parameters	Description	Values	Unit
V_a	Armature voltage	-	V
i_a	Armature current	-	A
e_b	Back EMF	-	(volts) V
$\tilde{\eta}_m$	Motor efficiency	$0.9 \approx 1$	-
κ_t	Motor torque constant	0.00767	Vs/rad
L_a	Inductance of armature	0.00018	H
R_a	Armature resistance	2.6	Ω
κ_g	Gear constant	3.71	-
κ_m	Motor constant	0.00767	Nm/A
r_g	Radius of gear	6.35×10^{-3}	m
$\tilde{\eta}_g$	Gear coefficient	$0.9 \approx 1$	-
λ	Amplifier gain	-	-
μ	Feedback amplifier gain	-	-

From figure (3.2) above the dynamic of the DC motor is governed by the following equation.

Using Kirchhoff's voltage law given by:

$$V_a = L_a \frac{di_a}{dt} + R_a i_a + e_b \tag{3.29}$$

Motor torque directly proportional to current: $\tau_m \;\alpha\; i_a$

$$\tau_m = \tilde{\eta}_m \kappa_t i_a \tag{3.30}$$

Armature inductance L_a is very small so we neglect (assume as zero for simplicity)

Then Eqn. (3.29) becomes

$$V_a = R_a i_a + e_b \tag{3.31}$$

The velocity of a tangent to the motor is the same as the cart's velocity. This provides the establishment of the relationship between a DC motor's back Emf and linear velocity.

$$\tilde{\omega} = \kappa_g \frac{\dot{x}}{r_g} \tag{3.32}$$

$$e_b = \kappa_m \tilde{\omega} = \kappa_m \kappa_g \frac{\dot{x}_1}{r_g} \tag{3.33}$$

Substitute Eqn. (3.32) and Eqn. (3.33) to Eqn. (3.31)

$$v_a = R_a i_a + \kappa_m \kappa_g \frac{\dot{x}_1}{r_g} \tag{3.34}$$

The relation between an input voltage and output torque is derived from Eqn. (3.34)

$$i_a = \frac{v_a r_g - \kappa_m \kappa_g \dot{x}_1}{r_g R_a} \tag{3.35}$$

Replace i_a in Eqn. (3.35) with the output torque of the DC motor in Eqn. (3.30)

$$\tau_m = \tilde{\eta}_m \kappa_t \left(\frac{v_a r_g - \kappa_m \kappa_g \dot{x}_1}{r_g R_a}\right) \tag{3.36}$$

We can't get the ideal torque we calculate in the equation because of the mechanical losses of the DC motor and gear efficiency. The actual torque at the input terminal is a small percentage of the torque produced by the DC motor.

$$\tau_g = \tilde{\eta}_g \tau_m \tag{3.37}$$

$$\tau_g = \tilde{\eta}_g \tilde{\eta}_m \kappa_t \left(\frac{v_a r_g - \kappa_m \kappa_g \dot{x}_1}{r_g R_a}\right) \tag{3.38}$$

The applied gear torque is converted into linear force F by a pinion with torque τ_m

$$\tau_g = F \times r_g \therefore F = \frac{\tau_g}{r_g} \tag{3.39}$$

Remember: we said that $F = u$

$$F = \frac{\tilde{\eta}_g \tilde{\eta}_m \kappa_t}{r_g} \left(\frac{v_a}{R_a} - \frac{\kappa_m \kappa_g x_2}{r_g R_a}\right) \tag{3.40}$$

The armature voltage control is shown in figure 3.3

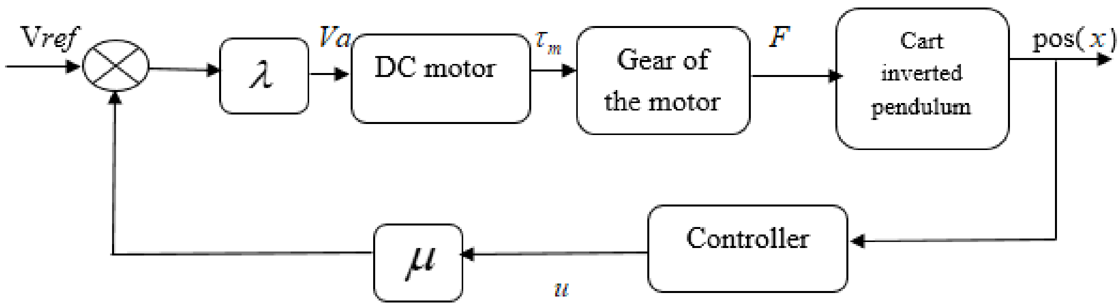

Figure 3. 4 Overall diagrams of DC motor

From the above Figure 3.3, the reference voltage can be variable i.e. zero or periodic. The DC motor's armature voltage, which serves as a voltage source, is the difference between the reference voltage and the signal from the controller. Moreover, the servo feedback gain λ is used to increase the intensity of the error signal.

$$V_a = \lambda(V_{ref} - \mu u) \tag{3.41}$$

Computing Eqn. (3.30) of V_a. The required force used to derive the cart is expressed with a reference signal (V_{ref}), control effort (u) and cart's velocity (x_2).

$$u = \frac{\tilde{\eta}_g \tilde{\eta}_m \kappa_t}{r_g} \left(\frac{\lambda (V_{ref} - \mu u)}{R_a} - \frac{\kappa_m \kappa_g x_2}{r_g R_a} \right) \tag{3.42}$$

$$u = \frac{\tilde{\eta}_g \tilde{\eta}_m \kappa_t \lambda V_{ref}}{R_a r_g} - \frac{\tilde{\eta}_g \tilde{\eta}_m \kappa_t \lambda \mu u}{R_a r_g} - \frac{\tilde{\eta}_g \tilde{\eta}_m \kappa_t \kappa_m \kappa_g x_2}{R_a r_g{}^2} \tag{3.43}$$

$$\left(1 + \frac{\tilde{\eta}_g \tilde{\eta}_m \kappa_t \lambda \mu}{R_a r_g}\right) u = \frac{\tilde{\eta}_g \tilde{\eta}_m \kappa_t \lambda V_{ref}}{R_a r_g} - \frac{\tilde{\eta}_g \tilde{\eta}_m \kappa_t \kappa_m \kappa_g x_2}{R_a r_g{}^2} \tag{3.44}$$

$$u = \frac{\dfrac{\tilde{\eta}_g \tilde{\eta}_m \kappa_t \lambda V_{ref}}{R_a r_g} - \dfrac{\tilde{\eta}_g \tilde{\eta}_m \kappa_t \kappa_m \kappa_g x_2}{R_a r_g{}^2}}{\left(1 + \dfrac{\tilde{\eta}_g \tilde{\eta}_m \kappa_t \lambda \mu}{R_a r_g}\right)} \tag{3.45}$$

To simplify the above equations let's use

$$\begin{aligned} \delta_1 &= \frac{\tilde{\eta}_g \tilde{\eta}_m \kappa_t \lambda}{R_a r_g} \\ \delta_2 &= \frac{\tilde{\eta}_g \tilde{\eta}_m \kappa_t \kappa_m \kappa_g}{R_a r_g{}^2} \\ \delta_3 &= 1 + \frac{\tilde{\eta}_g \tilde{\eta}_m \kappa_t \lambda \mu}{R_a r_g} \end{aligned} \tag{3.46}$$

$$u = \frac{\delta_1 V_{ref} - \delta_2 x_2}{\delta_3} \tag{3.47}$$

Eqn. (3.35) leads to the conclusion that current control is analogous. This equation demonstrates that the armature current is changed by the control signal by solving for the armature current i_a.

$$i_a = \frac{V_a}{R_a} - \frac{\kappa_m \kappa_g x_2}{R_a r_g} \tag{3.48}$$

Then substituting Eqn. (3.41) into Eqn. (3.48) yields,

$$i_a = \frac{\lambda(V_{ref} - \mu u)}{R_a} - \frac{\kappa_m \kappa_g x_2}{R_a r_g} \quad (3.49)$$

$$i_a = \frac{\lambda}{R_a} V_{ref} - \frac{\lambda\mu}{R_a} u - \frac{\kappa_m \kappa_g x_2}{R_a r_g} \quad (3.50)$$

If V_{ref} is zero, from Eqn. (3.50) the value of armature current i_a, is dependent on x_2 and u. As x_2 is a system variable, it is affected by u. This implies that armature current depends entirely on u,

$$i_a = -\frac{\lambda\mu}{R_a} u - \frac{\kappa_m \kappa_g x_2}{R_a r_g} \quad (3.51)$$

If there is no torque applied to the system then the armature current is zero also because it's directly proportional. (i.e. after disturbance is removed, rejected or compensated) the control signal is zero. As indicated in Eqn. (3.51), the control signal will be zero, since the linear velocity of the cart is zero under this condition.

$$0 = -\frac{\lambda\mu}{R_a} u - \frac{\kappa_m \kappa_g x_2}{R_a r_g} \quad (3.52)$$

$$u = -\frac{\kappa_m \kappa_g x_2}{\lambda \mu r_g} \quad (3.53)$$

We can use armature voltage controlled or armature current controlled via voltage source or current source to control the force applied to a cart also as in figure 3.2 If a servo amplifier is used, the only difference is that the control signal u is added as an additional current source in place of V_a as the input signal to the DC motor.

CHAPTER FOUR

CONTROLLER DESIGN

4.1 Subsystems of the Cart-Inverted Pendulum System

In this chapter, the dynamics of the cart inverted pendulum consider as two subsystems, namely the cart subsystem and the pendulum subsystem. Firstly, a backstepping controller is designed for the pendulum subsystem. Then a linear state feedback controller is applied to the cart subsystem. Finally, the two controllers are combined to produce the overall controller. As far as the main controller design is the hybrid of two linear and nonlinear controllers the backstepping state feedback is a nonlinear controller and for comparison LQR controller is used.

Cart subsystem

$$\dot{x}_1 = x_2 \tag{4.1}$$

$$\dot{x}_2 = \frac{(J+ml^2)mlx_4{}^2 \sin x_3 - m^2l^2 g \sin x_3 \cos x_3 + ml \cos x_3 b_p x_4 - (J+ml^2)b_{eq}x_2 + (J+ml^2)u}{D}$$

And,

Pendulum subsystem

$$\dot{x}_3 = x_4 \tag{4.2}$$

$$\dot{x}_4 = \frac{-m^2l^2x_4{}^2 \sin x_3 \cos x_3 + (M+m)mgl \sin x_3 + ml \cos x_3 b_{eq} x_2 - (M+m)b_p x_4 - ml \cos x_3 u}{D}$$

Where, $D = (J+ml^2)(M+m) - m^2l^2 \cos^2 x_3$

4.2 Backstepping Plus State Feedback Controller

4.2.1 Backstepping controller for the pendulum subsystem

The backstepping technique usually uses a back step design to gradually construct the Lyapunov function while designing the corresponding virtual controller. Among the most significant nonlinear control design methodologies, the backstepping design methodology has a wide range of applications. It was first presented by P. V. Kokotovic and his co-authors, (Krstic & Barbara, 1992),(*Kokotovic1992.Pdf*, n.d.). A nonlinear control technique founded on the Lyapunov theorem is the backstepping control strategy. Due to its systematic and recursive design methodology for nonlinear feedback control, the backstepping control design techniques have attracted a lot of interest.

The backstepping methodology offers a variety of design tools for accommodating nonlinearities and can prevent undesirable cancellations, in contrast to the feedback linearization method, which has issues with the accurate model need and the cancellation of valuable nonlinear elements. Due to its recursive usage of Lyapunov functions, backstepping has a design flexibility advantage over other control approaches. The main concept of the backstepping design is to recursively choose some suitable state variables as virtual inputs for lower dimension subsystems of the overall system and the backstepping design is based on the design of Lyapunov functions for each stable virtual controller.

Looking at Eqn. (4.2), it can be seen that the dynamics related to the rod rotation are separated from the dynamics of the cart position. A backstepping controller is designed based on the rotational dynamics of the rod as,

$$\dot{x}_3 = x_4 \tag{4.3a}$$

$$\dot{x}_4 = \frac{-m^2 l^2 x_4{}^2 \sin x_3 \cos x_3 + (M+m)mgl \sin x_3 + ml \cos x_3 b_{eq} x_2 - (M+m) b_p x_4 - ml \cos x_3 u_2}{D} \tag{4.3b}$$

Where u_2 is the control input when only the pendulum subsystem is considered.

Considering x_4 a virtual control w, Eqn. (4.3a) can be rewritten as

$$\dot{x}_3 = w \tag{4.4}$$

The Lyapunov stability is

$$v_1(x_3) = \frac{1}{2} x_3{}^2 \text{ (Quadratic and Positive definite (PD) on } \mathbb{R}\text{)} \tag{4.5}$$

$$\dot{v}_1 = x_3 \dot{x}_3 = x_3 w \tag{4.6}$$

If we choose virtual control w

$$w = -k_3 x_3 \text{ (} k_3 \text{ >0 is a design parameter)} \tag{4.7}$$

For backstepping control, we use the change of variables as

$$z = x_4 - w = x_4 + k_3 x_3 \tag{4.8}$$

Now x_2 is replaced by the new state z. Namely,

$$x_4 = z + w = z - k_3 x_3 \tag{4.9}$$

To transform the system Eqn. (4.3) into the form of (x_3, z), from Eqn. (4.3a) and Eqn. (4.3b),

$$\dot{x}_3 = x_4 = z - k_3 x_3 \tag{4.10}$$

Furthermore, differentiating Eqn. (4.6) and substituting Eqn. (4.3a) and Eqn. (4.3b) gives

$$\dot{z} = \dot{x}_4 + k_3 \dot{x}_3 \tag{4.11}$$

$$= [\frac{-m^2 l^2 x_4{}^2 \sin x_3 \cos x_3 + (M+m)mgl \sin x_3 + ml \cos x_3 b_{eq} x_2 - (M+m) b_p x_4 - ml \cos x_3 u_2}{D}]$$

$$+k_3(z - k_3 x_3)$$

In (x_3, z) coordinates, the system Eqn. (4.1) can be represented as follows:

$$\dot{x}_3 = z - k_3 x_3 \tag{4.12a}$$

$$\dot{z} = [\frac{-m^2 l^2 x_4{}^2 \sin x_3 \cos x_3 + (M+m)mgl \sin x_3 + ml \cos x_3 b_{eq} x_2 - (M+m) b_p x_4 - ml \cos x_3 u_2}{D}]$$

$$+ k_3(z - k_3 x_3)$$

(4.12b)

Next, we consider the Lyapunov function given by

$$v_2(x_3, z) = v_1(x_3) + \frac{1}{2} z^2 = \frac{1}{2}(x_3{}^2 + z^2) \tag{4.13}$$

We find that,

$$\dot{v}_2 = x_3 \dot{x}_3 + z\dot{z} \tag{4.14}$$

$$\dot{v}_2 = x_3(z - k_3x_3) +$$
$$z([\frac{-m^2l^2{x_4}^2 \sin x_3 \cos x_3 + (M+m)mgl \sin x_3 + ml \cos x_3 b_{eq} x_2 - (M+m)b_p x_4 - ml \cos x_3 u_2}{D}]$$
$$+k_3(z - k_3x_3))$$

(4.15)

If we choose the control law u_1 as

$$u_2 = \frac{1}{ml \cos x_3}[D(x_3 + k_4 z + k_3(z - k_3x_3)) + (M+m)mgl \sin x_3 - m^2l^2(z - k_3x_3)^2 \sin x_3 \cos x_3$$
$$+ml \cos x_3 b_{eq} - (M+m)b_p(z - k_3x_3)]$$

(4.16)

Where k_4 >0 is a user-defined parameter, then

$$\dot{v}_2 = -k_3{x_3}^2 - k_4 z^2 \quad (4.17)$$

It is clear $\dot{v}_2$ is globally Negative definite (ND) on $\Re^2$

The model is nonlinear with the pendulum angle when the system is moved up from the pending position to the upright position. The system's control problem is much more difficult than it appears to be for a variety of reasons, including the loss of geometric properties of the system when the pendulum moves through horizontal positions.

4.2.2 Linear State Feedback Controller for the Cart Subsystem

If the pendulum subsystem is properly controlled by the backstepping technique, the angle x_3 and the angular velocity x_4 approach zero, so the cart subsystem can be regarded as a linear model of

$$\dot{x}_1 = x_2$$
$$\dot{x}_2 = \frac{-(J+ml^2)b_{eq}x_2 + (J+ml^2)u_1}{D^{'}} \quad (4.18)$$

Where u_1 is the control input when only the cart subsystem is considered.

Equation (4.18) can be described in the state space form as

$$\dot{x} = A_m x + B_m u$$
$$y = C_m x \quad (4.19a)$$

$$A_m = \begin{bmatrix} 0 & 1 \\ 0 & \dfrac{-(J+ml^2)b_{eq}}{D'} \end{bmatrix}, B_m = \begin{bmatrix} 0 \\ \dfrac{J+ml^2}{D'} \end{bmatrix} \text{ and } C_m = \begin{bmatrix} 1 & 0 \end{bmatrix} \tag{4.19b}$$

Based on this subsystem model, a state feedback controller is designed. For driving the system states x_1 and x_2 from any initial states to the set point, the following tracking controller is used.

$$u_1 = -k_1(y - y_r) - k_2 x_2 \tag{4.20}$$

Where k_1 and k_2 are the user-defined state feedback gains so that all the poles of the closed-loop system have a negative real part.

4.2.3 Proposed Controller

In the previous sections, each controller for two subsystems was designed. The two controllers are combined to obtain the overall control input as

$$\begin{aligned} u &= u_1 + u_2 \\ &= -k_1(y - y_r) - k_2 x_2 + \frac{1}{ml\cos x_3}[D(x_3 + k_4 z + k_3(z - k_3 x_3)) \\ &\quad + (M+m)mgl\sin x_3 - m^2 l^2 (z - k_3 x_3)^2 \sin x_3 \cos x_3 \\ &\quad + ml\cos x_3 b_{eq} - (M+m) b_p (z - k_3 x_3)] \end{aligned} \tag{4.21}$$

Where k_1, k_2, k_3 and k_4 are the user-defined gains that determine the performance of the overall control system.

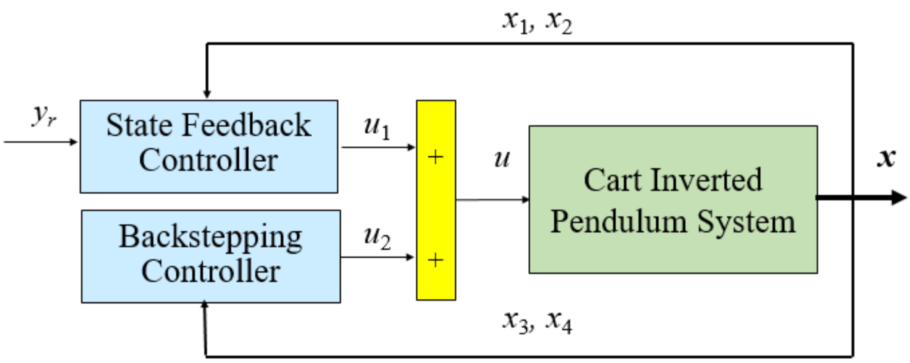

Figure 4. 1 Overall Structure of backstepping state feedback controller

4.3 Linear State Controller for the Performance Comparison

In this section, we design an optimal controller to stabilize the pendulum around zero states by using the linearized model in Equation (3.26). LQR is an optimal state feedback controller that calculates its state feedback gains by minimizing the error between the desired and actual states to zero according to the weights assigned to different states and inputs.

The results obtained with a linear quadratic controller are presented in this paper as compared with the main controllers. Since the optimization problem can be expressed in terms of the tracking errors and the cost function, the linearized model of the plant around the desired operating point can be used to develop a linear quadratic controller. The quadratic cost function is to be minimized.

$$J = \int_0^{\infty} [e(t)^T Q e(t) + u(t)^T R u(t)] dt \tag{4.22}$$

Where, $e = x_d - x$, $x_d = [y_r \ 0 \ 0 \ 0]^T$, $Q \in \Re^{n \times n}$ symmetric, positive semi-definite matrix is $R \in \Re^{m \times m}$ a positive definite weight matrix, usually, they are diagonal.

The control law is given by

$$u(t) = -Ke(t) \tag{4.23}$$

Where the optimal feedback gain matrix K is

$$K = R^{-1} B_m^T P \tag{4.24}$$

Where $\boldsymbol{P} \in \Re^{4 \times 4}$ denotes a positive definite symmetric constant matrix obtained from the steady-state solution of the Riccati differential equation

$$A_m{}^T P + P A_m - P B_m R^{-1} B_m^T P + Q = 0 \tag{4.25}$$

The proper selection of the weighting matrices is required for a successful controller design. Q is used to penalize the bad performance by minimizing the system states, while R is used for penalizing the control effort.

4.4 Genetic Algorithm Optimization

As mentioned above, the proposed controller has four gains that affect the overall system performance. Adjusting them properly becomes a multivariate optimization problem. To do this, a well-established optimization process is used to identify the best settings. In this case, the genetic algorithm (GA) is used to select the best values for the Backstepping state feedback parameters. The control parameters are computed in the algorithm by minimizing the fitness function given by the integral absolute error (IAE) performance index (Husain 2014).

Genetic Algorithm (GA) this type of algorithm uses mutation, inheritance, crossover, and selection, methods inspired by evolutionary biology to find solutions to problems. GA is a type of searching algorithm. It looks for an optimal solution to a problem in a solution space. The method of searching is a key feature of the GA (Yusuf, 2014), (Mansoor & Bhutta, 2016).

The algorithm generates a "population" of possible solutions to the problem and allows them to "evolve" over time to find better and better ones. The population is a set of candidate solutions that the algorithm considers. Over the generations of the algorithm, new members are "born" into the population, while others "die" out. The term "individual" refers to a single solution in a population. An individual's fitness is a measurement of how "good" the solution that the individual represents. The higher the fitness, the better the solution, of course, it is based on the problem to be solved.

GA is a technique based on natural evolution principles such as heredity, mutation, selection, and crossover. GA has demonstrated its ability to find near-optimal solutions to complex situations. However, it may require a long processing time to reach a near-optimal solution.

In the natural world, the survival of the fittest is similar to the selection process. Individuals are chosen for “cross-over” (breeding) based on their fitness values. The more fit an individual is, the more likely the individual will be able to reproduce. The cross-over happens when the two solutions are mixed to create two new individuals. Everyone has a small chance of mutating during each generation, which will modify the individual in some way. The algorithm ends when the population has attained a suitable fitness level or a maximum number of generations has been produced. If the method has finished due to the maximum number of generations, a good solution may have been found. The genetic optimization algorithm is used in Matlab either in code or the GA optimization toolbox app.

4.6 Performance Tests

The closed-loop performance of the designed control system is measured based on a performance index. In this work, the following evaluation called the integral of absolute error and control (IAEU) is used:

$$IAEU = \int_0^{\infty} (|e(t)| + \eta\,|\,u(t)\,|)dt \tag{4.26}$$

Where, $e(t)$ is the difference between the set point and the output with $y_r(t)–y(t)$ and η is the weighting factor. This performance index is particularly useful for suppressing unnecessarily excessive control effort at the expense of a slower response through the proper use of η. In this thesis, η is set to 0.1.

4.7 Swing up of Cart Inverted Pendulum

Cart inverted pendulum has no internal creation of energy in the system rather it generates energy during the swinging up of the pendulum. the passivity-based method exploits the fact that the pendulum is the dissipative system the storage of energy of the system is E the system less than or equal to the sum of available storage energy E_0 at the initial time plus the total energy $\int_0^t \lambda(w)dw$ supplied to the system from external sources in the interval $[0,t]$ equation (4.27) gets mathematically.

$$E - E0 \leq \int_0^t \lambda(w)dw \tag{4.27}$$

The dissipative nature of the cart's inverted pendulum makes it possess a trajectory where the total energy of the system is zero. Such a trajectory is the homoclinic orbit that joins the saddle equilibrium point (upright position) to itself. The swing-up control tasks, therefore, lie in designing the control action to take the system to this homoclinic orbit by using the appropriate Lyapunov function. The orbits of this phase plot are determined by constant energy contours for a basic pendulum phase picture. The Homoclinic Orbit is a particularly unique orbit that goes via an unstable fixed point, in figure 4.1 the Red orbit is the Homoclinic orbit.

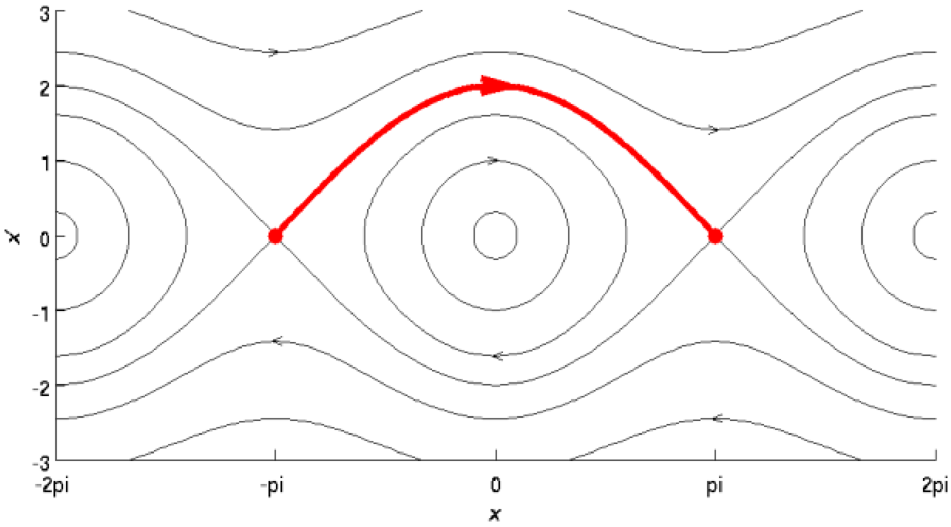

Figure 4. 2 phase portraits of cart inverted pendulum motion

In the mathematical modelling in chapter three Eqn. (3.24) derived from Euler Lagrangian's underactuated mechanical system form. From that moment of inertia and pendulum friction is negligible for the swing-up design because it was so small.

Then,

$$M(q)\ddot{q} + C(q,q)\dot{q} + G(q) = \tau \tag{4.28}$$

$$M(q) = \begin{bmatrix} M+m & ml\cos\theta \\ ml\cos\theta & ml^2 \end{bmatrix}, C(q,q) = \begin{bmatrix} 0 & -ml\sin\theta\dot{\theta} \\ 0 & 0 \end{bmatrix}, \quad G(q) = \begin{bmatrix} 0 \\ -mgl\sin\theta \end{bmatrix} \text{and}$$

$$\tau = \begin{bmatrix} F - b_{eq}\dot{x} \\ 0 \end{bmatrix} \tag{4.29}$$

To check the passivity of the system it is evaluated the derivative of the total energy of the system $\dot{E}$ and checked if it satisfies the mathematical condition passivity condition of Eqn. (4.27)

Note that $M(q)$ is symmetric, and $\det(M(q)) = (M+m)(ml^2) - (ml\cos\theta)^2 > 0$

$$= Mml^2 + m^2l^2\sin^2\theta > 0 \tag{4.30}$$

Therefore, $M(q)$ is positive definite for all q from Eqn. (4.26) and Eqn. (4.27). It follows that

$$M - 2C = \begin{bmatrix} 0 & ml\sin\theta\dot{\theta} \\ -ml\sin\theta\dot{\theta} & 0 \end{bmatrix} \tag{4.31}$$

Which is a skew-symmetric matrix. An important property of skew-symmetric matrices, which will be used in establishing the passivity property of the inverted pendulum is,

$$\chi^T(M(q) - 2C(q,q))\chi = 0 \quad \forall \chi \in \Re^2 \tag{4.32}$$

The potential energy of the pendulum can be defined as $PE = mgl(\cos\theta - 1)$

Note that PE this is related to

$$G(q) = \frac{\partial PE}{\partial q} = \begin{bmatrix} 0 \\ -mgl\sin\theta \end{bmatrix} \tag{4.33}$$

4.7.1 Passivity-Based control of the Cart-Inverted Pendulum

The total energy of the cart inverted pendulum system is given by

$$E = KE(q,\dot{q}) + PE \tag{4.34}$$

$$= \frac{1}{2}\dot{q}^T M(q)\dot{q} + mgl(\cos\theta - 1) \tag{4.35}$$

Therefore from Eqn. (4.28)-(4.32), we obtain

The derivative $\dot{E}$ becomes

$$\dot{E} = \frac{\partial}{\partial t}(KE(q,\dot{q})) + \frac{\partial}{\partial t}(PE) \tag{4.36}$$

$$\dot{E} = \frac{\partial}{\partial t}(\frac{1}{2}\dot{q}^T M(q)\dot{q}) + \frac{\partial}{\partial t}(PE)\dot{q} \tag{4.37}$$

$$\dot{E} = \dot{q}^T M(q)\ddot{q} + \frac{1}{2}\dot{q}^T \dot{M}(q)\dot{q} + \dot{q}^T G(q) \tag{4.38}$$

$$E = \dot{q}^T(M(q)\ddot{q}\frac{1}{2}\dot{M}(q)\dot{q}) + \dot{q}^T G(q)) \tag{4.39}$$

From Eqn. (4.26) $M(q)\ddot{q} = -C(q,q)\dot{q} - G(q) + \tau$ and substitute in above Eqn. (4.37)

$$E = \dot{q}^T(-C(q,\dot{q})\dot{q} - G(q) + \tau + \frac{1}{2}\dot{M}(q)\dot{q}) + \dot{q}^T G(q)$$

Here Eqn. (4.30) is mainly used to simplify

$$E = \dot{q}^T(\dot{M}(q) - 2C(q,\dot{q}))\dot{q} + \dot{q}^T\tau$$

$$= \dot{q}^T\tau = \dot{x}u \tag{4.40}$$

Integrating both sides of the above equation (4.38)

$$E(t) - E(0) = \int_0^t \dot{x}u dt \tag{4.41}$$

$E(t)$ is maximum energy at an upright position $(\theta = \pi)$ that potential energy $mgl(\cos\pi - 1) = -2mgl$

$$-2mgl - E(0) \le \int_0^t \dot{x}u dt \tag{4.42}$$

Therefore, the system has u input and $\dot{x}$ output that is passive

Note that for $u = 0$ and $\theta \in [0, 2\pi]$, the system Eqn. (4.26) has the subset of two equilibrium points: $(x, \dot{x}, \theta, \dot{\theta}) = (x_d{}^*, 0, 0, 0)$ an unstable equilibrium point and $(x, \dot{x}, \theta, \dot{\theta}) = (x_d{}^*, 0, \pi, 0)$ a stable equilibrium point. For unstable equilibrium points and $-2mgl$ stable equilibrium points, the total energy E is equal to zero. The control objective is to stabilize the system around its unstable equilibrium point, i.e. to bring the pendulum to its upper position and cart displacement to zero simultaneously.

4.7.2 Stabilization in the vicinity of the homoclinic orbit

Let us first note that because of Eqn. (4.34) and Lagrangian equation, if $\dot{x} = 0$ and $E = 0$ then,

$$\frac{1}{2}ml^2\dot{\theta}^2 = mgl(1 - \cos\theta) \tag{4.43}$$

The given equation defines a very particular trajectory, which corresponds to a homoclinic orbit. Note that $\dot{\theta} = 0$ if only if $\theta = 0$. This means that the pendulum's angular position moves clockwise or counter clockwise until it reaches the equilibrium point $(\theta, \dot{\theta}) = (0,0)$. Thus our objective can be reached if the system can be brought to the orbit Eqn. (4.43) for $\dot{x} = 0, x = 0$ and $E = 0$. Bringing the system to this homoclinic orbit solves the problem of "swinging up" the pendulum. The control must eventually be changed to a controller that ensures the equilibrium's asymptotic stability to balance the pendulum at the top equilibrium point. We ensure that the trajectory will reach the basin of attraction of any linear balancing controller by ensuring convergence to the aforesaid homoclinic orbit.

Our goal is now to design a controller that is attracted to homoclinic orbit considering the Lyapunov equation. The passivity property of the system suggests the use of the total energy E in Eqn. (4.35) in the controller design. Since we wish to bring it to zero $x, \dot{x} \;\; E$, we propose the following Lyapunov function candidate

$$V(q,\dot{q}) = \frac{1}{2}\kappa_e E^2 + \frac{1}{2}\kappa_\upsilon \dot{x}^2 + \frac{1}{2}\kappa_x x^2 \tag{4.44}$$

Where $\kappa_e, \kappa_\upsilon$ and κ_x are strictly positive constraints. Note that $V(q,\dot{q})$ this is a positive semi-definite function. Differentiating V and using Eqn. (4.40),

We obtain

$$\frac{\partial V}{\partial t} = \kappa_e \frac{\partial E}{\partial t} + \kappa_\upsilon \frac{\partial \dot{x}}{\partial t} + \kappa_x \frac{\partial x}{\partial t} \tag{4.45}$$

$$\dot{V} = \kappa_e E\dot{E} + \kappa_\upsilon \dot{x}\ddot{x} + \kappa_x x\dot{x} \tag{4.46}$$

Substituting Eqn. (4.40) in the above Eqn. (4.46)

$$\dot{V} = \kappa_e E\dot{x}u + \kappa_\upsilon \dot{x}\ddot{x} + \kappa_x x\dot{x} \tag{4.47}$$

Collecting the same terms

$$\dot{V} = \dot{x}(\kappa_e Eu + \kappa_\upsilon \ddot{x} + \kappa_x x) \tag{4.48}$$

From standard robotic form $M(q)\ddot{q} + C(q,\dot{q})\dot{q} + G(q) = \tau$

Let us now compute $\ddot{x}$ from chapter three in Eqn. (3.23a) and Eqn. (3.23b) the inverse $M(q)$ can be obtained from Eqn. (4.29) is given by,

$$M(q)^{-1} = \frac{1}{\det M(q)} \begin{bmatrix} ml^2 & -ml\cos\theta \\ -ml\cos\theta & M+m \end{bmatrix} \tag{4.49}$$

Where $\det M(q)$ is defined in Eqn. (4.30), therefore,

$$\begin{bmatrix} \ddot{x} \\ \ddot{\theta} \end{bmatrix} = \frac{1}{Mml^2 + m^2l^2\sin^2\theta} \begin{bmatrix} ml^2 & -ml\cos\theta \\ -ml\cos\theta & M+m \end{bmatrix} \left(\begin{bmatrix} ml\sin\theta\dot{\theta} + u \\ mgl\sin\theta \end{bmatrix} \right) \tag{4.50}$$

$$\begin{bmatrix} \ddot{x} \\ \ddot{\theta} \end{bmatrix} = \frac{1}{Mml^2 + m^2l^2\sin^2\theta} \begin{bmatrix} m^2l^3\sin\theta\dot{\theta}^2 - m^2l^2g\sin\theta\cos\theta + ml^2u \\ (M+m)mgl\sin\theta - ml\cos\theta - m^2l^2\dot{\theta}^2\sin\theta\cos\theta \end{bmatrix} \tag{4.51}$$

$$\ddot{x} = \frac{m^2l^3\sin\theta\dot{\theta}^2 - m^2l^2g\sin\theta\cos\theta + ml^2u}{Mml^2 + m^2l^2\sin^2\theta} \tag{4.52a}$$

$$\ddot{\theta} = \frac{(M+m)mgl\sin\theta - ml\cos\theta - m^2l^2\dot{\theta}^2\sin\theta\cos\theta}{Mml^2 + m^2l^2\sin^2\theta} \tag{4.52b}$$

Then taking Eqn. (4.52a) and substituting in Lyapunov equation in Eqn. (4.47)

$$\dot{V} = \dot{x}(\kappa_e Eu + \kappa_\upsilon \left(\frac{m^2l^3\sin\theta\dot{\theta}^2 - m^2l^2g\sin\theta\cos\theta + ml^2u}{Mml^2 + m^2l^2\sin^2\theta} \right) + \kappa_x x) \tag{4.53}$$

Cancelling out ml^2 in denominator and numerator of $\ddot{x}$

$$\dot{V} = \dot{x}(\kappa_e Eu + \kappa_\upsilon \left(\frac{m\sin\theta(l\dot{\theta}^2 - g\cos\theta) + u}{M + m\sin^2\theta} \right) + \kappa_x x) \tag{4.54}$$

$$\dot{V} = \dot{x}(\left(\kappa_e E + \frac{\kappa_\upsilon}{M + m\sin^2\theta} \right) u + \kappa_\upsilon \left(\frac{m\sin\theta(l\dot{\theta}^2 - g\cos\theta)}{M + m\sin^2\theta} \right) + \kappa_x x) \tag{4.55}$$

We propose a control law such that

$$\left(\kappa_e E + \frac{\kappa_\upsilon}{M + m\sin^2\theta} \right) u + \kappa_\upsilon \left(\frac{m\sin\theta(l\dot{\theta}^2 - g\cos\theta)}{M + m\sin^2\theta} \right) + \kappa_x x = -\kappa_\ell \dot{x} \tag{4.56}$$

Then the Lyapunov function becomes a negative definite

$$\dot{V} = -\kappa_\ell \dot{x}^2 \tag{4.57}$$

Note that for other functions u that $\dot{x}u > 0$ are also possible the control law in Eqn. (4.56) will have no singularities, proving that

$$\left(\kappa_e E + \frac{\kappa_\upsilon}{M + m\sin^2\theta}\right) \neq 0 \tag{4.58}$$

Note from Eqn. (4.35) $E \geq -2mgl$. Thus Eqn. (4.34) always holds if the following inequality is satisfied

$$\frac{\kappa_\upsilon}{\max_\theta (M + m\sin^2\theta)} > 2mgl\kappa_e \tag{4.59}$$

This gives the following lower bound for $\dfrac{\kappa_\upsilon}{\kappa_e}$

$$\frac{\kappa_\upsilon}{\kappa_e} > 2mgl(M+m) \tag{4.60}$$

Note that when using the control law in Eqn. (4.32), the pendulum can get stuck at the lower or stable equilibrium point $(x, \dot{x}, \theta, \dot{\theta}) = (0, 0, \pi, 0)$ to avoid this singular point, which occurs when $E = -2mgl$. We require

$$|E| < \vartheta = 2mgl \tag{4.61}$$

Since V is a non-increasing function in Eqn. (4.57), (4.61) will hold if the initial conditions are such that

$$V(0) < \kappa_e \frac{\vartheta^2}{2} \tag{4.62}$$

In the above equation, it imposes bounds on the initial energy of the system .note that the potential energy $PE = mgl(\cos\theta - 1)$ lies between $-2mgl$ and 0. This means that the initial kinetic energy should belong to $[0, \vartheta + 2mgl]$.

Note also that the initial position of the cart $x(0)$ is arbitrary since it can always choose an appropriate value for κ_x V Eqn. (4.62). It $x(0)$ is large, we should choose a small one κ_x. The convergence rate of the algorithm may however decrease when κ_x is small.

Note that when initial kinetic energy $KE(q(0),\dot{q}(0))$ is zero, the initial angular position $\theta(0)$ should belong $(-\pi,\pi)$. This means that the only forbidden point is $\theta(0)=\pi$. When initial kinetic energy $KE(q(0),\dot{q}(0))$ is different from zero, i.e. $KE(q(0),\dot{q}(0))$ belongs to $[0,\vartheta+2mgl]$, an initial angular position $\theta(0)$ that can even be pointing downwards, i.e. $\theta(0)=\pi$ provided that $KE(q(0),\dot{q}(0))$ is not zero.

Even though our controller is local, its basin of attraction is far from small.

$$u=\frac{\kappa_{\upsilon} m\sin\theta(g\cos\theta-l\dot{\theta}^2)-M+m\sin^2\theta(\kappa_x x+\kappa_{\ell}\dot{x})}{\kappa_e E(M+m\sin^2\theta)+\kappa_{\upsilon}} \tag{4.63}$$

CHAPTER FIVE

RESULT AND DISCUSSION

This chapter discusses the proposed Backstepping state feedback controller for the cart inverted pendulum through simulation and analysis. In addition, for the comparison purpose, the LQR controller is designed and also energy-based passivity of the pendulum controller is used for swinging up a controller and optimally tuned using a GA MATLAB simulation and Simulink is used to get results.

In this chapter, the devotion is to the show results that come from the controllers used for cart inverted pendulum stabilization and also swing-up.in addition to that performance of controllers is also discussed, regarding settling time, overshoot, rise time and *IAE*.

5.1 Tuning using Genetic algorithm

A genetic algorithm is one of the evolutionary optimization tools. In this thesis, 50 maximum iterations are used to get the best optimum result. The Upper bound and lower bound used are

$$LB = \begin{bmatrix} -15 & -15 & 0 & 0 \end{bmatrix}$$
$$UB = \begin{bmatrix} 0 & 0 & 15 & 25 \end{bmatrix}$$

Figure 5.1 shows the tuning optimization of the control system using the genetic algorithm.

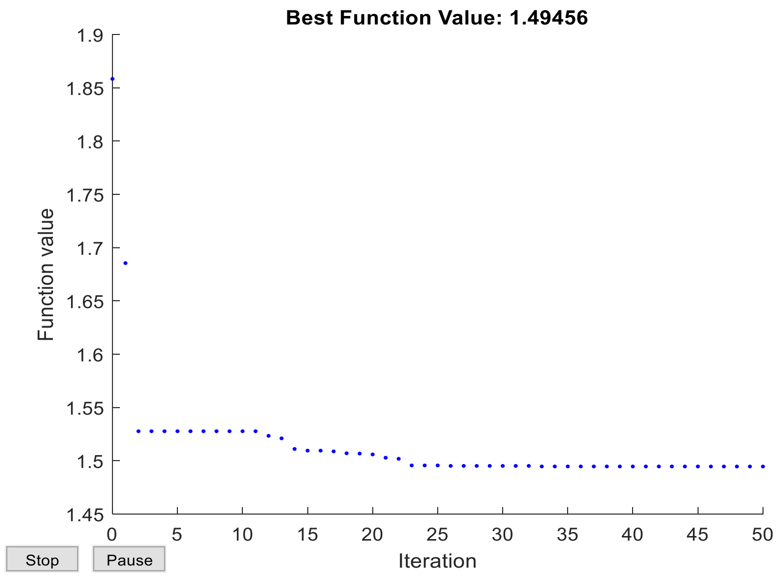

Figure 5. 1 Tuning optimization of Genetic Algorithm

5.2 Controller Settings

The proposed controller designed in chapter four tuned by GA has four parameters thus $\left[k_1 = -11.4164 \quad k_2 = -10.5235 \quad k_3 = 4.4350 \quad k_4 = 21.8965\right]$ with 0.1 weighting factor of optimization.

As mentioned in the previous chapter, LQR provides control input in terms of minimizing the quadratic performance index, Q and R are user-defined weighting matrices that affect the overall performance. The higher the state error term, the faster the closed-loop response becomes and the more oscillation it has due to bigger control input, whereas the higher the actuator effort term, the slower the closed-loop response becomes with less oscillation.

$$Q = \begin{bmatrix} 5 & 0 & 0 & 0 \\ 0 & 1 & 0 & 0 \\ 0 & 0 & 3 & 0 \\ 0 & 0 & 0 & 1 \end{bmatrix} \text{ and } R = 0.1$$

With this selection Q and R we got a controller gain matrix

$$\tilde{k} = [-7.0711 \quad -8.2701 \quad -51.9844 \quad -11.0440]$$

In this section, a set of simulation works are done using MATLAB based on four performance tests, that is, set point changes, multiple set point changes, parameter uncertainty and disturbance rejection tests. The performances of the proposed controller are compared with those of the backstepping state feedback and LQR controllers. The regulation performance is measured in terms of the peak time (t_p), rise time (t_r), settling time (t_s), overshoot (M_p) and IAE. The more general challenge is to guide the pendulum from any arbitrary initial point to upright equilibrium and stabilize the cart in the desired position.

5.3 Discussion of Set Points Change Responses

A cart inverted pendulum set point change is used for upright stability; the stability is determined by the cart position and pendulum angle. Rising time (t_r), settling time (t_s), overshoot (M_p), and performance index IAE are used to evaluate the properties of set point change output. The proposed backstepping state feedback and LQR controllers are compared in this section. Set point change performance was compared with four scenarios:

- **Scenario 1:** (-1, 0, pi/4, 0) According to this scenario, the set point change response is implemented when the cart is about 1m to the left and the angle of the pendulum is pi/4, then regulating both the cart's position to reference position and the angle of the pendulum to zero.

- **Scenario 2:** (-1, 0, -pi/4, 0) the set point change response according to this scenario is implemented when the cart is about 1m to the left and the angle of the pendulum is -pi/4 both are left direction in the worst case to control and then regulating both the cart to reference position and angular position of a pendulum to zero.
- **Scenario 3:** (1, 0, -pi/4, 0) the set point change response according to this scenario is implemented when a cart is about 1m to the right and the angle of a pendulum is -pi/4 then regulating both carts to reference position and angular position of a pendulum to zero.
- **Scenario 4:** (1, 0, pi/4, 0) the set point change response according to this scenario is implemented when a cart is about 1m to the right and the angle of the pendulum is pi/4 both of them are in the same direction to the right due to this it’s the worst case and then regulating both cart’s to reference position and angular position of a pendulum to zero.

5.3.1 Response to Scenario 1

Based on this scenario, the set point change response of the proposed controller and LQR is shown in figure 5.2

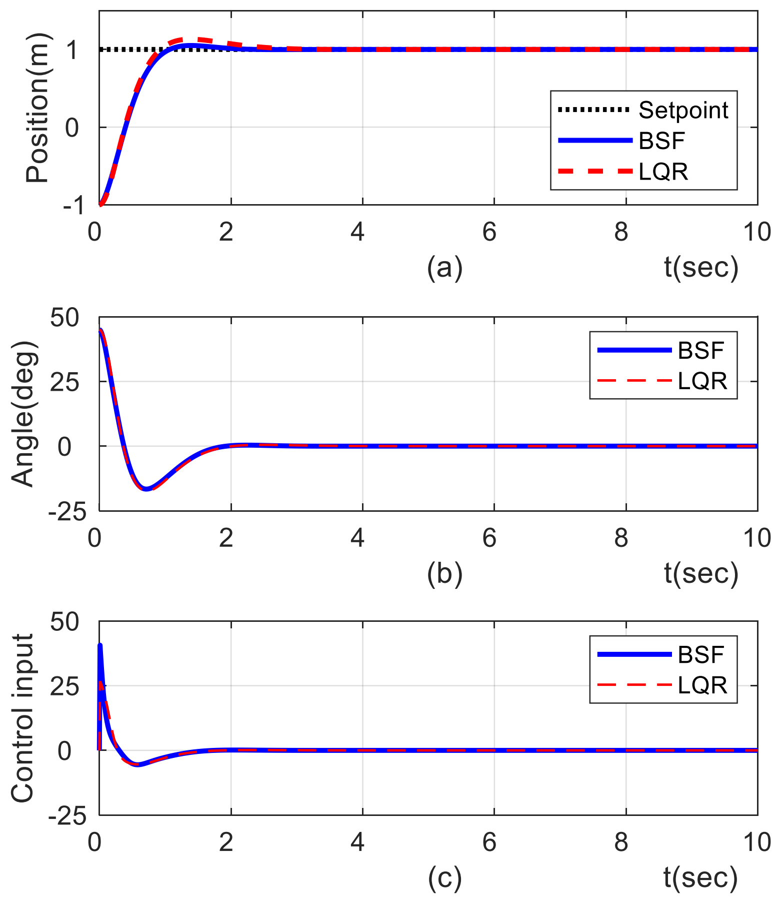

Figure 5. 2Response of set point change of scenario 1

As shown in the above figure (5.2) (a) cart position is started from -1m is set to point and reached the desired position of the cart its reference is 0m and also (b) shows the angle of the pendulum starting from 45 degrees it goes to 0 degree which is in the upright position. (c) Shows a control input U which drives the cart to move and to make the pendulum to an upright position.

Table 5.1 Set Point Tracking Scenario 1 Response

	t_s	t_r	M_p	IAE
BSF	1.6195	0.6644	2.5340	9.6278
LQR	2.3226	0.6023	6.5898	9.7726

As shown in table (5.1) the proposed method of backstepping state feedback shows a better performance than LQR. It has a 25.3% overshoot but LQR has 65.8% which is too much. As well as the proposed method has a 1.6195 sec settling time while the comparison controller has a 2.3226 sec settling time. In addition, IAE has better performance for backstepping state feedback controller which is 9.6278.

5.3.2 Response to Scenario 2

Based on this scenario, the set point change response of the proposed controller and LQR is shown in figure 5.3

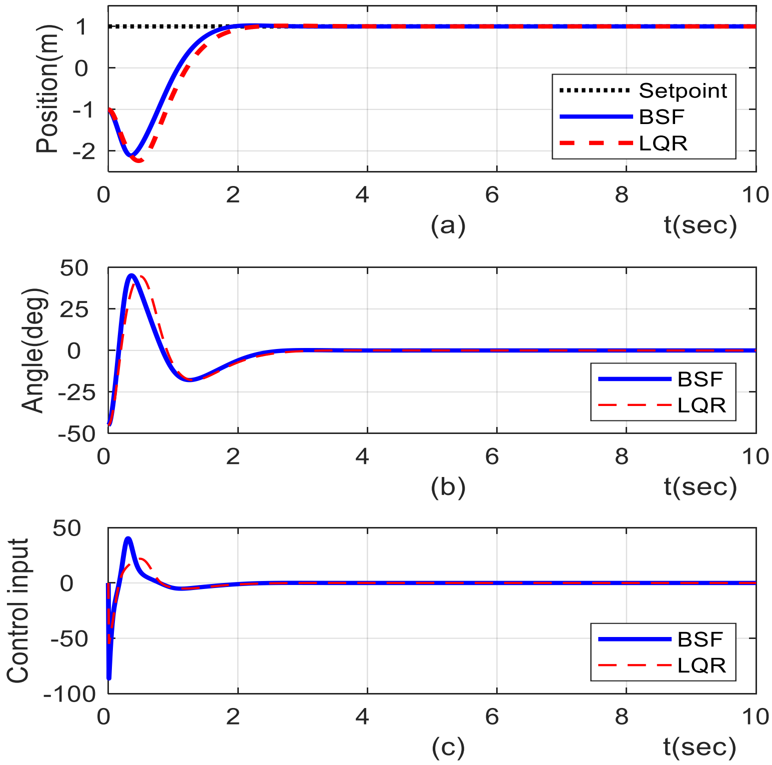

Figure 5. 3 Response of set point change of scenario 2

As shown in the above figure (5.3) (a) cart position is started from -1m is the set point and reached the desired position of the cart its reference is 1m and also (b) shows an angle of the pendulum starting from -45 degree it goes to 0 degree which is in the upright position (c) Shows a control input U which drives the cart to move and to make the pendulum to the upright position.

Table 5.2 Set Point Tracking Scenario 2 Response

	t_s	t_r	M_p	IAE
BSF	1.7417	0.7130	1.1622	10.0620
LQR	2.0148	0.7948	0.8761	10.1798

As shown in Table (5.2) the proposed method of backstepping state feedback shows a better performance than LQR. It has a 116.2% overshoot but LQR has 87.6% which is too much. This is because this scenario is the worst to control. As well as the proposed method has a 1.7417 sec settling time while the comparison controller has a 2.0148 sec settling time. In addition, IAE has better performance for backstepping state feedback controller which is 9.6278.

5.3.3 Response to Scenario 3

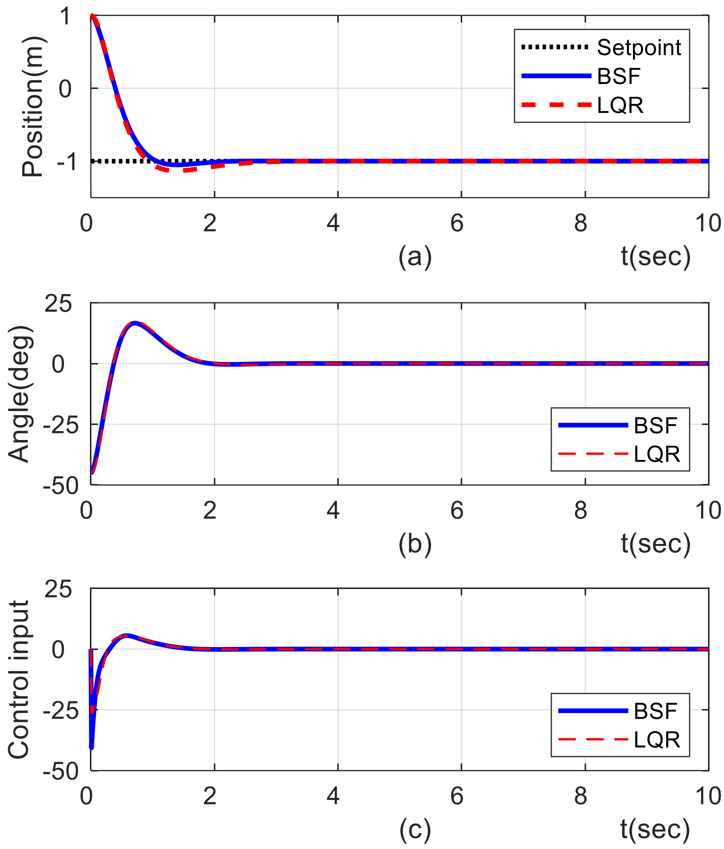

Figure 5. 4 Response of set point change of scenario 3

As shown in figure (5.4) above (a) the cart position is started from 1m is the set point and reached the desired position of the cart its reference is 1m and also (b) shows an angle of the pendulum starting from -45 degree it goes to 0 degree which is in an upright position. (c) Shows a control input u which drives the cart to move and to make the pendulum to the upright position.

Note: it has the same performance as scenario 1. Almost all properties assessed are equal.

5.3.4 Response to Scenario 4

Based on this scenario, the set point change response of the proposed controller and LQR is shown in figure 5.5

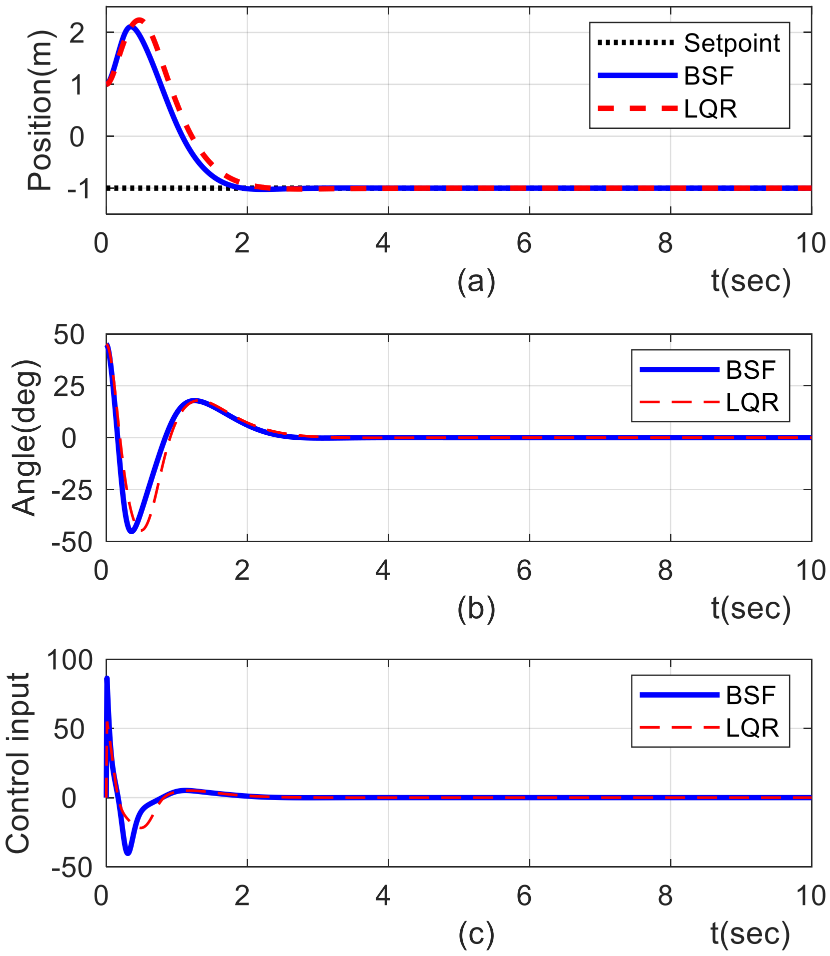

Figure 5. 5 Response of set point change of scenario 4

As shown in figure (5.5) above (a) the cart position started from -1m is the set point and reached the desired position of the cart its reference is 1m and also (b) shows an angle of the pendulum starting from -45 degree it goes to 0 degree which is in the upright position. (c) Shows a control input U which drives the cart to move and to make the pendulum to the upright position.

Note: it has the same performance as scenario 1. Almost all properties assessed are equal

5.4 Discussion of disturbance rejection responses

In cart inverted pendulum gust disturbance is taken as disturbance it is assumed 10% of control effort and that is applied to 4-6 sec when a system is running. A set of simulations based on two scenarios from the above scenario 1 and 3 were performed to demonstrate the proposed method's disturbance rejection performance.

$d = \pm 5$ is added as an external excitation to the cart inverted pendulum system during the time interval $t \in [4, 6]$sec to test the robustness of the proposed control approach the obtained simulation results are depicted in the figures below. it can be noticed that despite the existing uncertainties and the considered external disturbance the controller can steer the system to its desired values. It can be seen that our control design is robust to tolerate significant variation in the system parameters as well as the external disturbances

- Scenario 1: (-1, 0, pi/4, 0) while reference point yr is 1 and $\pm$10% of maximum control effort is assumed that $dw = 5$ so when it is negative it's down condition and when it's positive it is up condition.
- Scenario 3 (1, 0,-pi/4, 0) while the reference point yr is -1 and $\pm$10% of maximum control effort is assumed that $dw = 5$ so when it is negative it's down condition and when it's positive it's up condition.

5.4.1 Response to Scenario 1

The response of the two methods is performed when the disturbance dw is -5 or 5 around a time of 4-6 sec. unfortunately, the reference point yr is 1m. A graphical result is plotted for the proposed method of backstepping state feedback and LQR as shown in Figures 5.5 and 5.6 for up and down cases. As a result, the proposed method has better disturbance rejection than the compared method. Even though it has some effects due to disturbance, the effect of disturbance is eliminated after a moment and the position returns to the desired position due to control effort.

The performance parameters of settling time (t_s), pick time (t_p), recovery time (t_{recy}), overshoot (M_p), and IAE are used to compare controllers in the case of a disturbance rejection response. According to the simulation results, the proposed backstepping state feedback controller has a recovery time of 2.0507 seconds and an overshoot of 25.34% per cent. Table 5.3 lists the additional parameters. When the disturbance is considered, the proposed method has better performance parameter results, as shown by the graphical and tabular results.

Case 1: UP

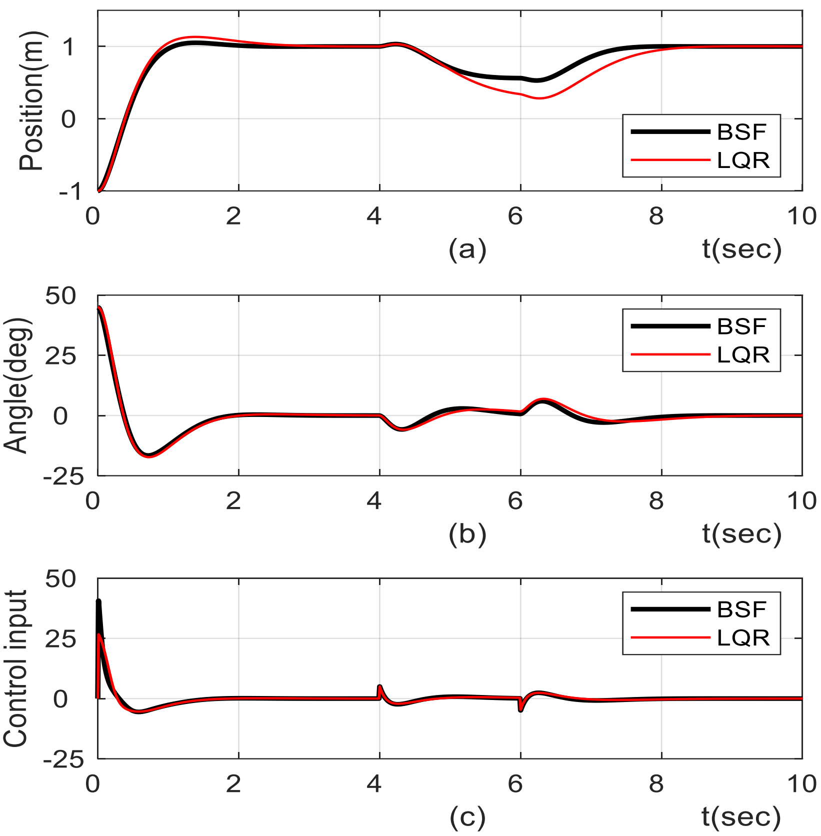

Figure 5. 6 Response of disturbance rejection in scenario 1 for up case

As shown in the above figure 5.6 (a) cart position has better disturbance rejection than the proposed method. (b) The angle of the pendulum has some effects due to disturbance after 6 sec also but it converges to zero degrees. At (c) shows a control effort has some distortion during the disturbance.

Table 5. 3 Response of Disturbance Rejection Response for Scenario 1 up a Case

	t_p	t_s	t_{recy}	M_p	IAE
BSF	1.3900	7.3691	2.0507	2.534	8.7519
LQR	1.3800	8.0516	2.1318	6.5898	8.3590

Case 2: Down

Down case means nothing but when $dw = 5$.figure below and table show the performance of controllers.

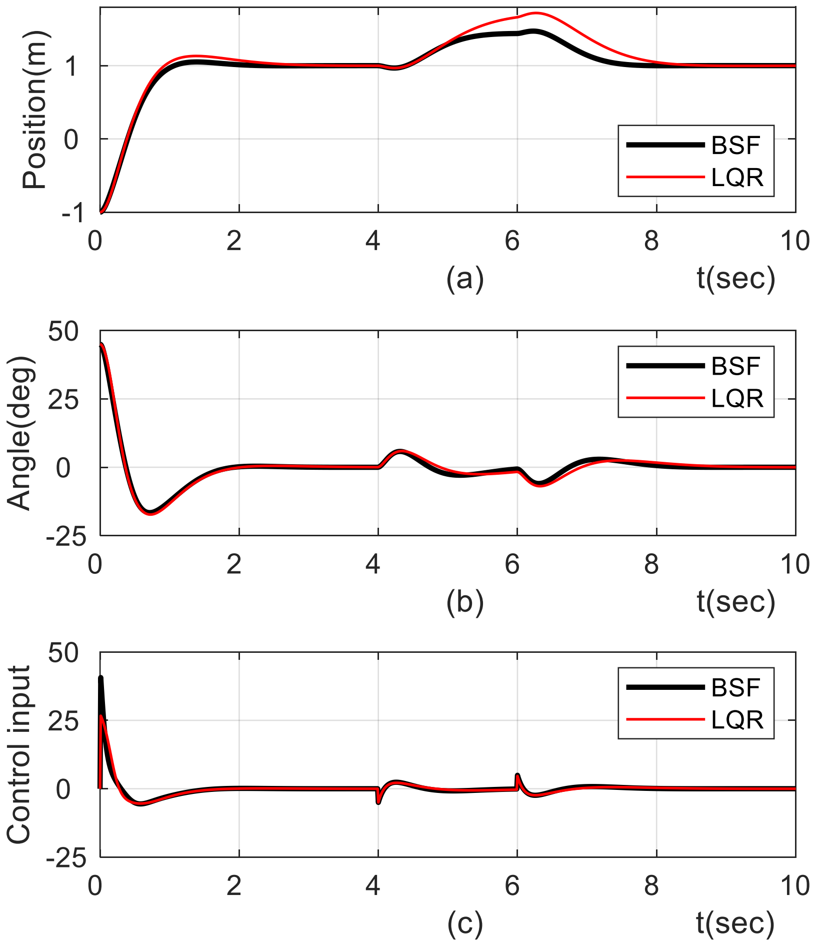

Figure 5. 7 Response of disturbance rejection in scenario 1 for down case

Table 5. 4 Performance of Scenario 1 Case Down

	t_p	t_s	t_{recy}	M_p	IAE
BSF	6.2300	7.3671	2.4715	23.5771	10.5037
LQR	6.2700	8.0516	2.7187	35.9367	11.1863

5.4.2 Response to scenario 3

The response of the two methods is performed when the disturbance dw is -5 or 5 around a time of 4-6 sec. unfortunately, the reference point yr is -1m. A graphical result is plotted for the proposed method of backstepping state feedback and LQR as shown in Figures 5.8 and 5.8 for up and down cases. Even though it has some effects due to disturbance, the effect of disturbance is eliminated after a moment and the position returns to the desired position due to control effort.

Case 1:UP

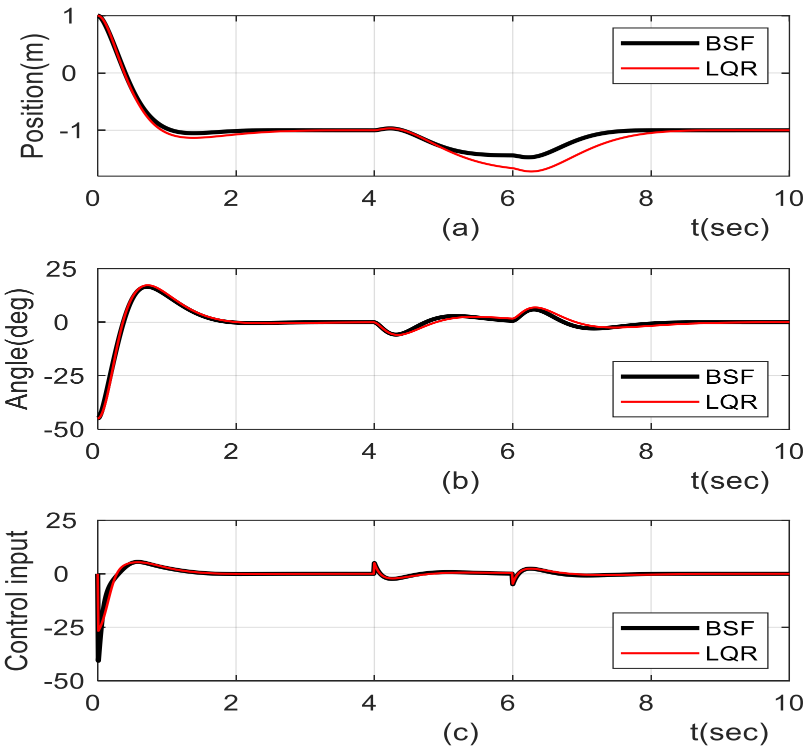

Figure 5. 8 Response of disturbance rejection in scenario 3 for up case

The performance parameters of settling time (t_s), pick time (t_p), recovery time (t_{recy}), overshoot (M_p), and IAE are used to compare controllers in the case of a disturbance rejection response. According to the simulation results, the performance is the same as scenario 1 with a down case. When the disturbance is considered, the proposed method has better performance parameter results, as shown by the graphical and tabular results.

Case 2: Down

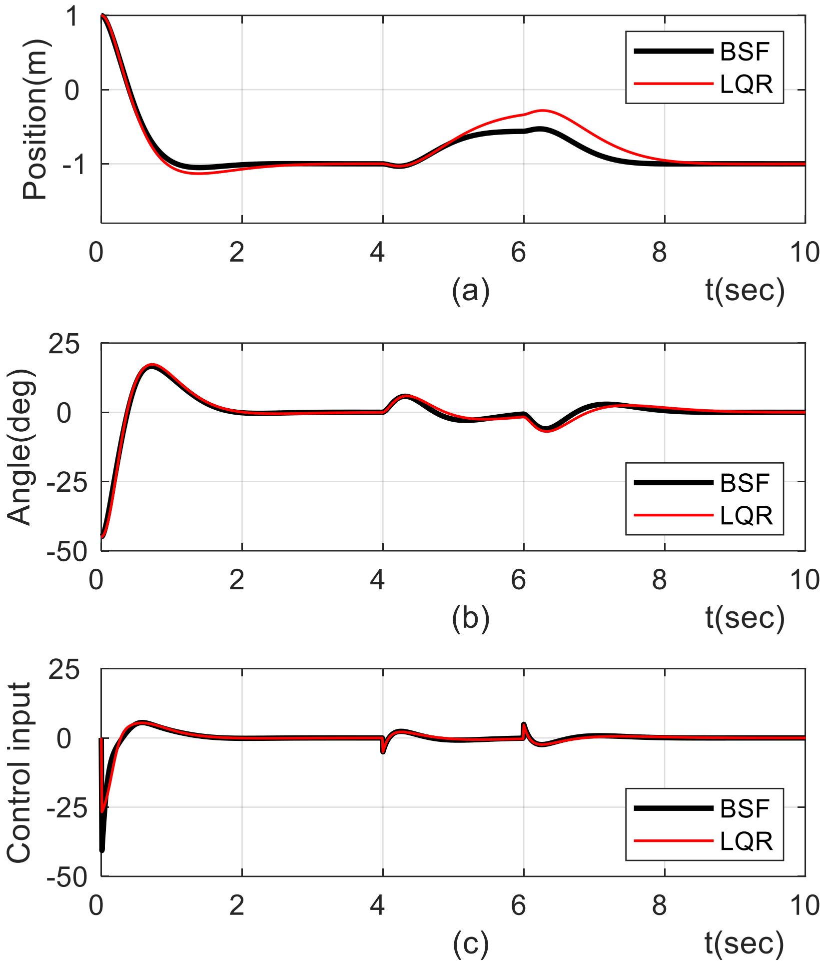

Figure 5. 9 Response of disturbance rejection in scenario 3 for down case

5.5 Multiple Set Point changes (MSP)

Here in this performance test we are checking various set points and letting the controller regulate. In the same situations in section 5.2, we are going to check for all four scenarios discussed above.

5.5.1 Response of MSP to scenario 1

Though we can see scenario 1 in figure 5.9 below (a) shows the position of the cart start with a reference of -1m to the left and goes back to 1m until it reaches 10 sec then the cart travels to -2m to left. When time is between 10 sec and 20 sec the cart is moving to 2m to right then while a cart is moving into 30 sec it goes back to -1m then after that it regulates finally to the origin.

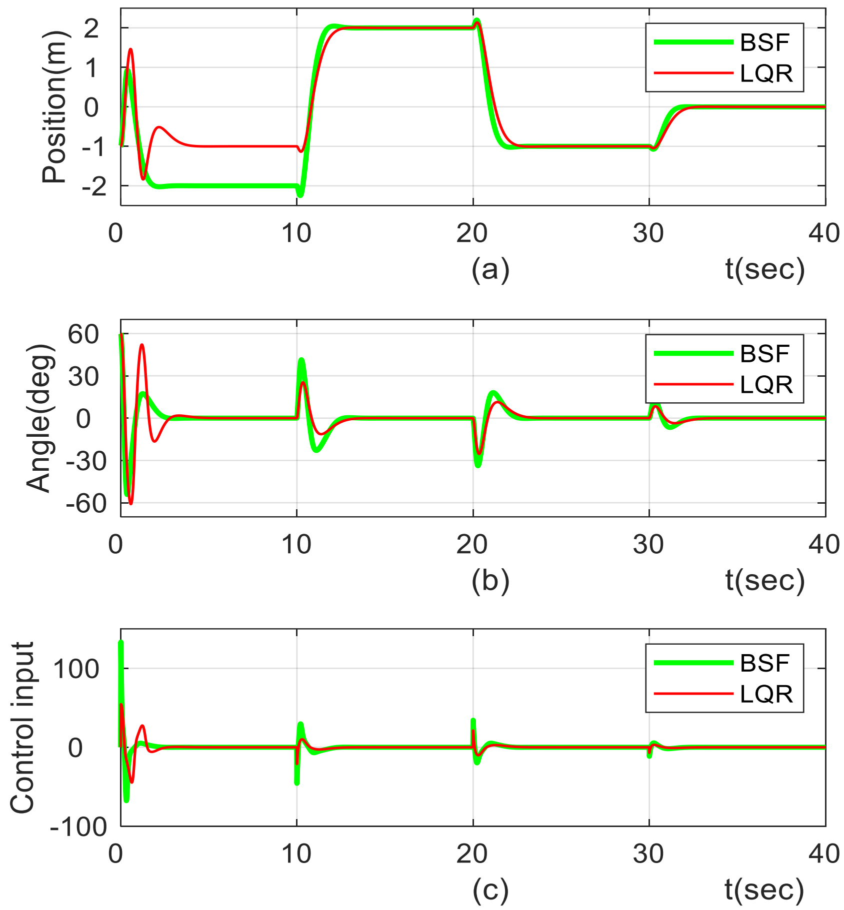

Figure 5. 10 Response of multiple set point change in scenario 1

Figure 5.10 (b) also shows what happened to the angle of the pendulum during multiple set point changes. The reference angle is pi/3 (60 degrees), when the cart starts moving the angles go back to -50 degrees then in a few seconds it becomes 15 degrees then up to 10 sec the angle regulate to 0deg then again when the cart set point is changing angle becomes swing comes to around 50 degrees then back to -15 degree and later it regulates. Again when the cart set point change is 2m to -1m the angle again deteriorates to 5 degrees then back to -5 degrees then it goes to the origin.

5.4.2 Response of MSP to scenario 2

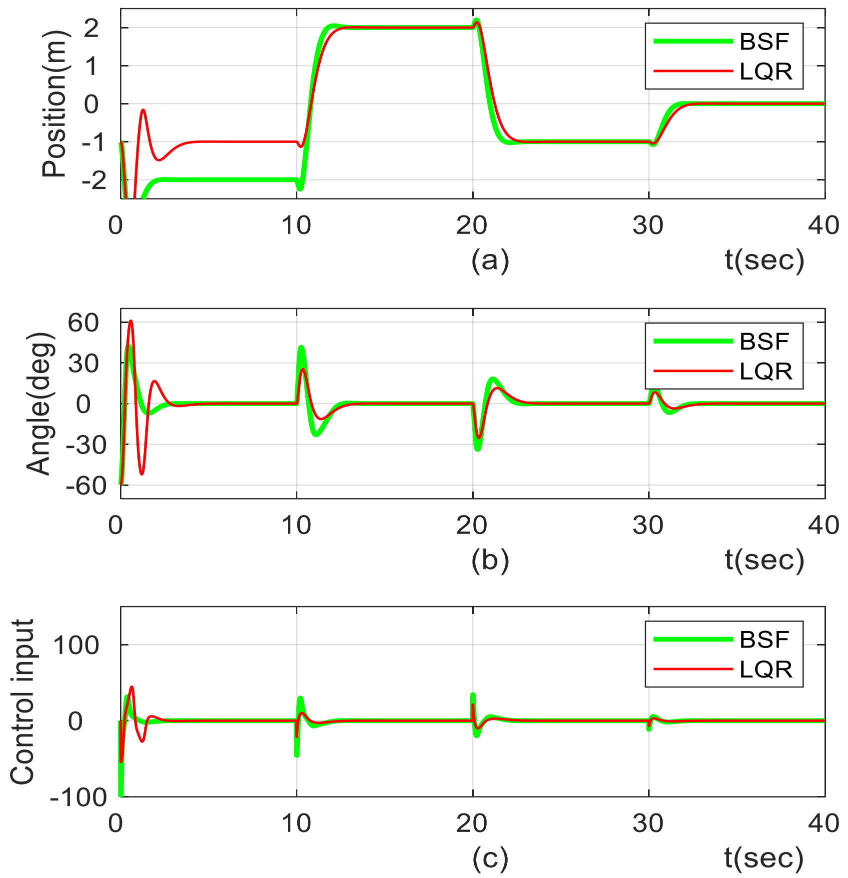

Figure 5. 11 Response of multiple set point change in scenario 2

5.4.3 Response of MSP to scenario 3

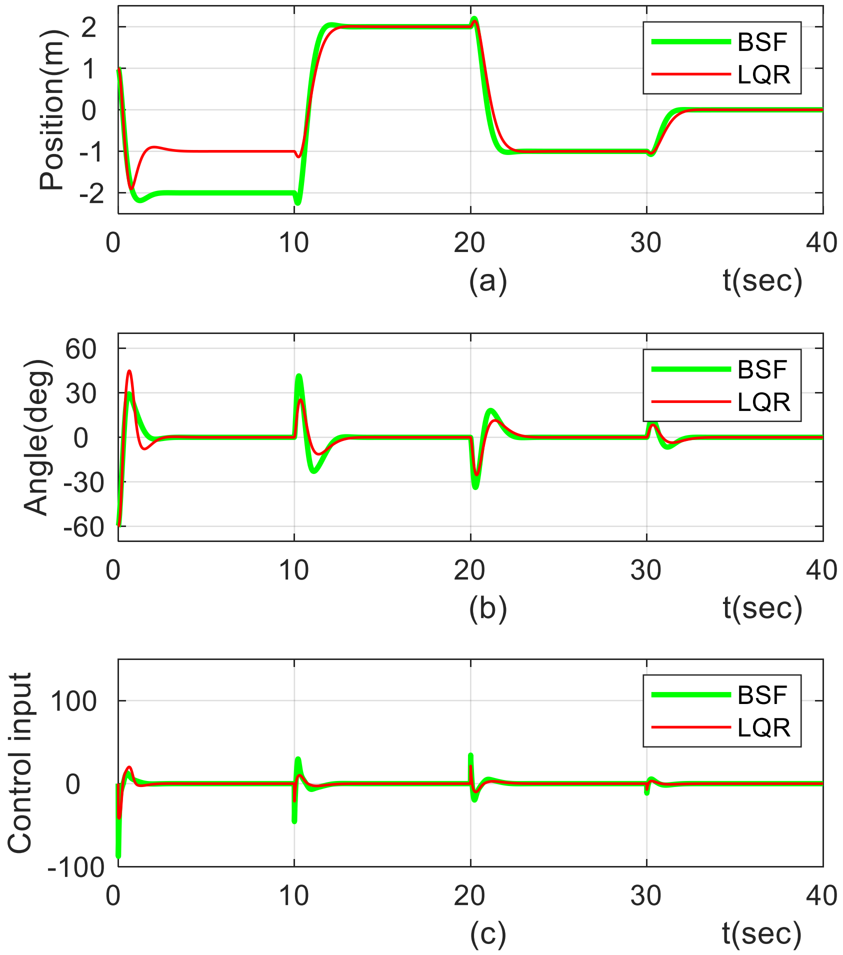

Figure 5. 12 Response of multiple set point change in scenario 3

5.4.4 Response to MSP to scenario 4

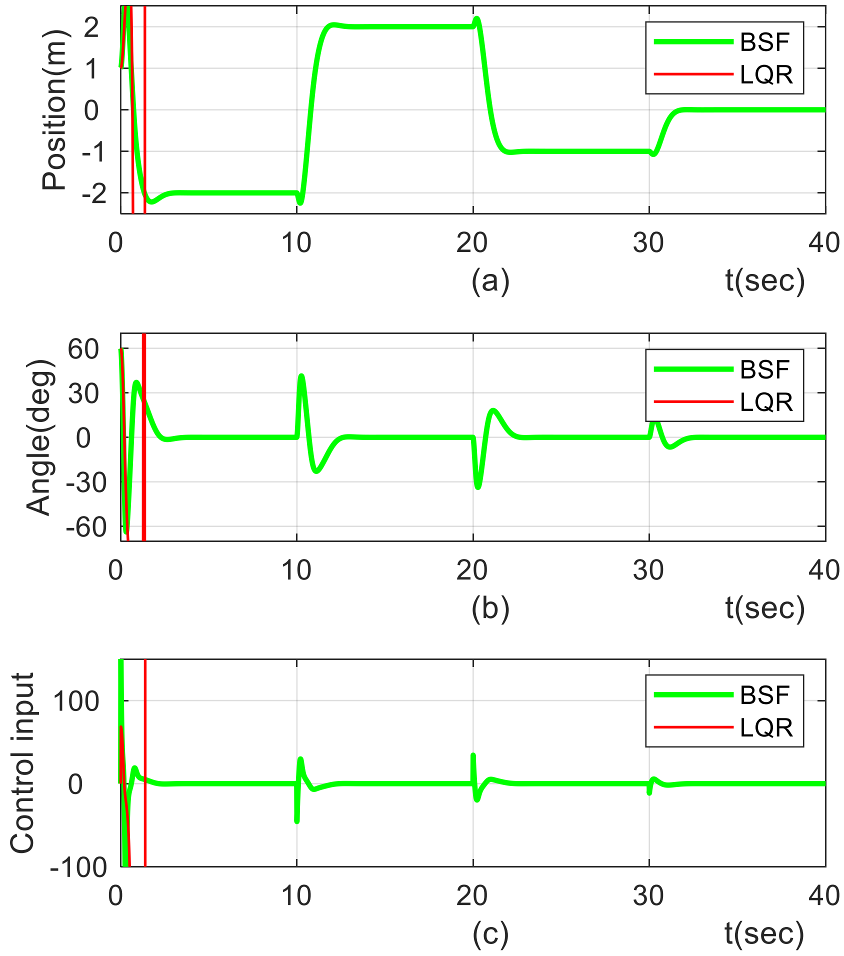

Figure 5. 13 Response of multiple set point change in scenario

From the above response of multiple set point changes in four scenarios the proposed backstepping state feedback controller can work faithfully. We can see the performances of the controllers using assessing indices such as overshoot (M_p) and IAE . Although the graph shows more we use some tabular forms to illustrate more.

Table 5.5 Performance Test of Multiple Set Point Change in All Scenarios

	Scenario 1		Scenario 2		Scenario 3		Scenario 4	
	M_p	IAE	M_p	IAE	M_p	IAE	M_p	IAE
BSF	41.8908	38.7655	111.00	51.0128	45.2646	39.4351	63.26	49.5474
LQR	62.370	48.2622	123.25	40.7678	62.37	49.3930	Inf	Inf

From the above table, we can see that the backstepping state feedback controller works in all scenarios but LQR completely fails.

Finally, what we can conclude from multiple set point changes is at the worst conditions case 2 and case 4 LQR is not efficient for the system rather backstepping state feedback (BSF) is working effectively in all scenarios.

5.6 Parameter Uncertainty

The proposed controller is more robust to parametric change than the LQR controller as it is shown in figure 5.14 below.

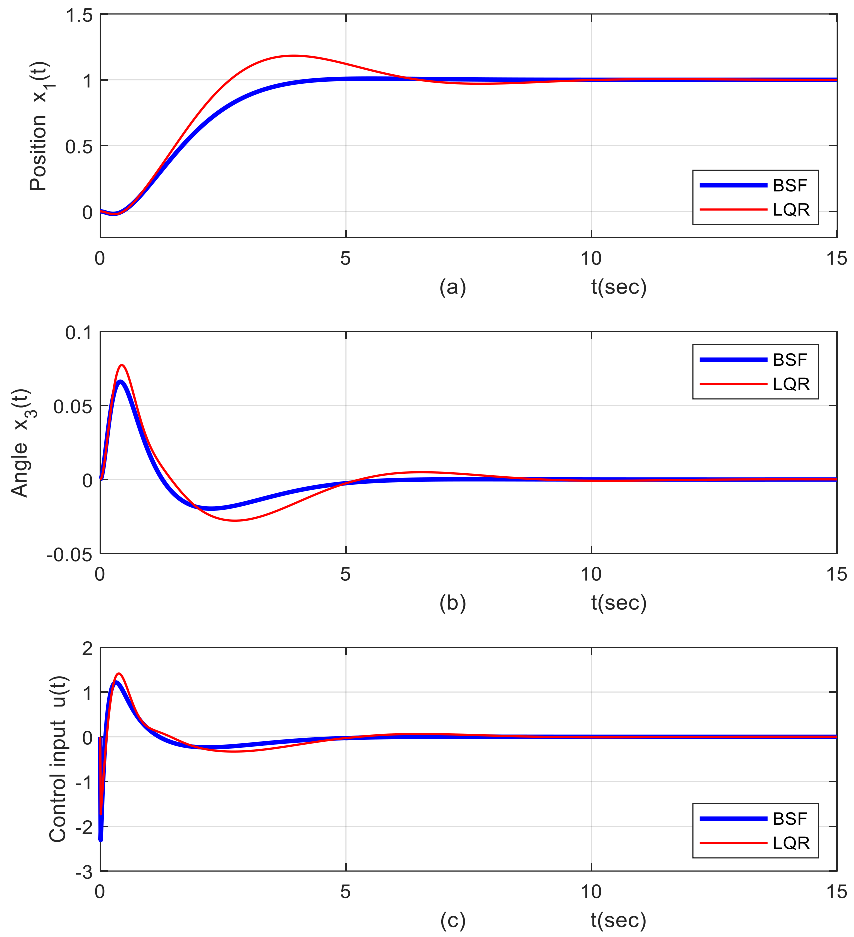

Figure 5. 14 Response to parametric uncertainty of controllers

Table 5.6 Parametric Uncertainty of Controllers

	t_r	t_s	t_p	M_p	IAE	IAU
BSF	2.3634	3.9734	5.5200	0.9216	1.8535	1.3106
LQR	1.6040	8.7285	3.9400	18.3082	1.7619	3.9400

5.7 Response of Energy-Based Passivity of Swing-up Control

Swing-up control is a very challenging zone of cart inverted pendulum to control. The classic energy-based controller is used in passivity swing-up control for the effectiveness of control. Then in this thesis, the proposed stabilizing controller GA tuned Backstepping state feedback controller is combined with energy-based passivity swing-up controller.

$$u_{control} = u_{swing} + u_{stab}$$

Control effort of swing up $u_{swing} = \dfrac{\kappa_{\upsilon} m \sin\theta (g\cos\theta - l\dot{\theta}^2) - M + m\sin^2\theta(\kappa_x x + \kappa_{\ell}\dot{x})}{\kappa_e E(M + m\sin^2\theta) + \kappa_{\upsilon}}$

Control effort of stabilization is also a combination of a backstepping state feedback controller

$$u_{stab} = -k_1(y - y_r) - k_2 x_2 + \frac{1}{ml\cos x_3}[D(x_3 + k_4 z + k_3(z - k_3 x_3)) + (M+m)mgl\sin x_3$$
$$-m^2 l^2 (z - k_3 x_3)^2 \sin x_3 \cos x_3 + ml\cos x_3 b_{eq} - (M+m) b_p (z - k_3 x_3)]$$

The parameters of the proposed stabilization control are mentioned in the above section, the swing-up control parameters are κ_{υ} =5.723, κ_x =13, κ_e =4 and κ_{ℓ} =0.9.

From figure 5.15 below pendulum swings at increasing amplitude from an original position of 180 degrees (3.14 *rad*) until it reaches 25 degrees (0.436 *rad*) where the switchover to stabilizing controller backstepping state feedback is done.

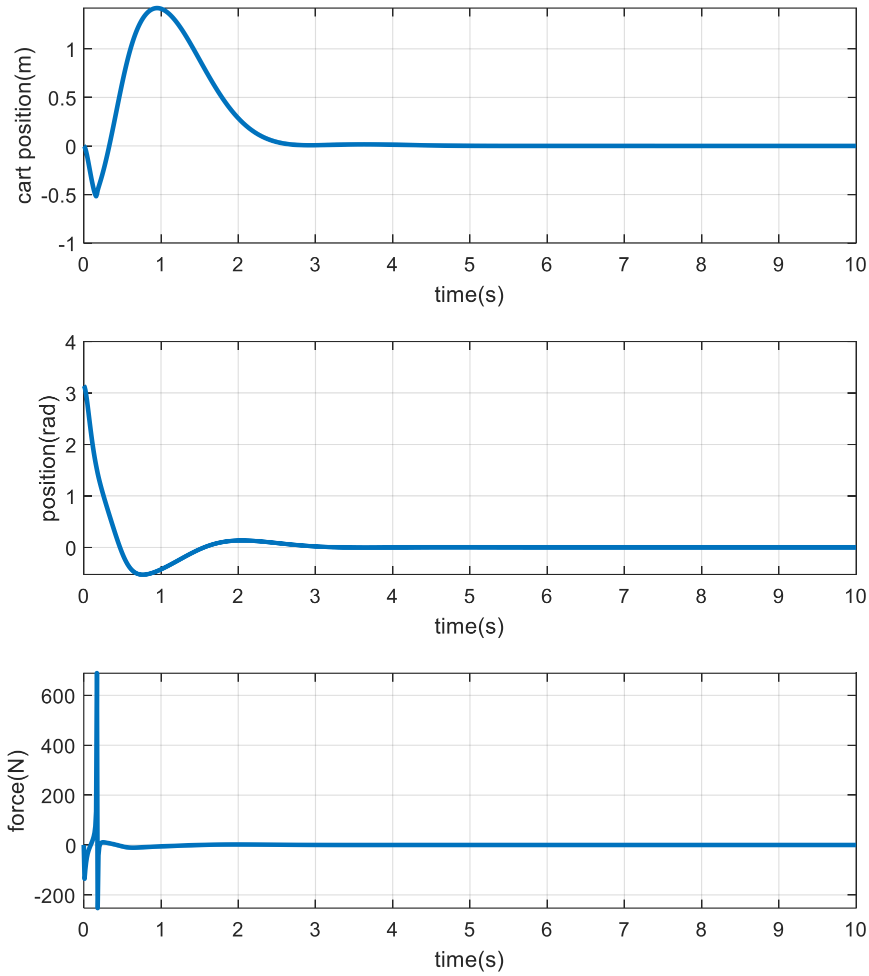

Figure 5. 15 Response of energy-based passivity swing-up control with BSF controller

It is shown in the figure below that swings up occur quickly and the proposed controller stabilizes the system in less than 1 second. The energy of the pendulum can be seen from the figure to approach zero from the value of -2 mgl after short seconds. The control action used in the system is a maximum of 0.68KN. The cart position varies from -0.5 meters to 1.42 meters then back to the origin at 2.49 seconds. The pendulum could be swung up to around 2.25 degrees (0.03898 rad) of the vertical equilibrium position using this swing-up controller, which was observed to have a wider domain of attraction. This controller can therefore be combined with any stabilizing controller in a hybrid control structure to swing up the cart inverted pendulum.

CHAPTER SIX

CONCLUSION AND RECOMMENDATION

6.1 Conclusion

In this thesis, the application of a nonlinear backstepping state feedback controller on a cart inverted pendulum system for stabilization problem and an energy-based passivity controller to swing up of the pendulum problem. The cart inverted pendulum is regarded as the combined system of the cart subsystem and pendulum subsystem. The Energy based passivity swing-up controller swing the pendulum from its pendant position to the inverted position, and the backstepping state feedback controller is used to stabilize the cart's inverted pendulum to the upright position. The proposed designed controller has been found to have a wider basin of attraction to the upright equilibrium and better use of control energy when close to the equilibrium point than compared LQR controller. The simulation results show promising results under set point change and multiple set point changes in different scenarios, with parameter uncertainty of 40% in figure 5.15 and disturbance applying up to ± 5 for applying backstepping state feedback controller.

According to the pendulum subsystem, the nonlinear controller is created using a backstepping design, but since the cart's displacement cannot be controlled, the state feedback controller combines with backstepping, which can control the cart's displacement and speed, and as a result, a stable nonlinear controller for the cart's inverted pendulum is generated. The parameters of the controller are tuned using the genetic algorithm optimization technique. The proposed controller is compared with the linear quadratic regulator (LQR) controller, and it is to show how it is effective. The performance of the controller is shown by settling time, overshoot, rise time and also the performance index of IAE.

6.2 Recommendation

This thesis introduces combined controllers of backstepping state-feedback for stabilization of a cart inverted pendulum and energy-based passivity control for swinging up the pendulum. The parameters used for designing a controller are randomly selected as stated in the above chapter but it is recommended to design in a systematic way of selecting system parameters. Since the proposed controller is more effective than the compared controller it implements that using controllers combined with other controllers is gaining the benefit of both controllers. To enhance the work done, combining backstepping controllers with other nonlinear, intelligent or adaptive controllers to make them more efficient. It is also recommended to utilize the actual system to implement the controllers developed for this thesis since it only used software simulation to assess the validity and performance of the controllers on the system.

Research fund Acknowledgment

Research is funded by Adama Science and Technology University under the grant number **ASTU/SM-R/573/22**, Adama, Ethiopia.

References

Boubaker, O. (n.d.). *The inverted Pendulum : A fundamental Benchmark in Control Theory and Robotics*.

Chaudhary, A. (2018). *Design of a Sliding Mode Controller (SMC) based on Reaching Law*. *182*(10), 45–49.

Christensen, J. H., & Christiansen, R. (2017). *Swing Up and Stabilisation of an Inverted Pendulum on a Cart using Nonlinear Methods*. *June*.

Coşkun, S. (2020). *Non-linear Control of Inverted Pendulum*. *35*(March), 27–38.

Cox, B. (2005). *Feedback Stabilization of Inverted Pendulum Models*.

Ebrahim, A., & Murphy, G. V. (n.d.). *Adaptive Backstepping Controller Design of an Inverted Pendulum*. 172–174.

Fernando Henrique Gomes Zucatelli, & Magno Enrique Mendoza Meza. (2015). Backstepping controllers for a cart-pole system in two configurations. *Proceedings of the 23rd ABCM International Congress of Mechanical Engineering*, *1*(1). https://doi.org/10.20906/cps/cob-2015-1292

Finoki, E., Nerguizian, V., & Saad, M. (2015). *Simulation of Non-Linear Flight Control Using Backstepping Method*. *182*, 1–8.

Fossen, T. I. (2019). *FEEDBACK LINEARIZATION CONTROL FOR SYSTEMS WITH MISMATCHED UNCERTAINTIES VIA DISTURBANCE OBSERVERS*. *21*(4), 1–13. https://doi.org/10.1002/asjc.1802

Fu, Y., & Lin, J. (2005). *Nonlinear Backstepping Control Design of the Furuta Pendulum*. 96–101.

Housner, G. W. (1963). The behavior of inverted pendulum structures during earthquakes. *Bulletin of the Seismological Society of America*, *53*(2), 403–417. https://doi.org/10.1785/bssa0530020403

Jörgl, M., Schlacher, K., & Gattringer, H. (2013). *Passivity based control of a cart with inverted pendulum*. *332*, 339–344. https://doi.org/10.4028/www.scientific.net/AMM.332.339

Kalyoncu, M. (2016). *Optimal Tuning of a LQR Controller for an Inverted Pendulum Using the Bees Algorithm*. *December*. https://doi.org/10.18178/joace.4.5.384-387

Khati, A. (2020). *Backstepping Control of Two Degrees of Freedom (2-DOF) Robot Manipulator*. *9*(4), 27–33.

Khudhair, M. Y., Hassan, M. Y., & Kadhim, S. K. (2021). *Backstepping Control Strategy* *for Overhead Crane System Backstepping Control Strategy for Overhead Crane System*. *September*. https://doi.org/10.30684/etj.v39i3A.1738

kokotovic1992.pdf. (n.d.).

Krafes, S., Chalh, Z., & Saka, A. (2016). *Review : Linear, nonlinear and intelligent controllers for the inverted pendulum problem*. *2*.

Krstic, K. M., & Barbara, S. (1992). *[; I*. 3276–3280.

Kumar, R., Singh, R. B., & Das, J. (2013). *MODELING AND SIMULATION OF INVERTED PENDULUM SYSTEM USING MATLAB : OVERVIEW*. 52–55.

Kurode, S., Chalanga, A., & Bandyopadhyay, B. (2011). Swing-up and stabilization of Rotary Inverted Pendulum using sliding modes. In *IFAC Proceedings Volumes (IFAC-PapersOnline)* (Vol. 44, Issue 1 PART 1). IFAC. https://doi.org/10.3182/20110828-6-IT-1002.02933

Lee, K. U., Choi, Y. H., & Park, J. B. (2017). Backstepping-based formation control of quadrotors with the state transformation technique. *Applied Sciences (Switzerland)*, *7*(11). https://doi.org/10.3390/app7111170

Lemos, E. (2018). *DC Motor Modeling and Control by using Backstepping Technique*. *December*.

Lim, Y. Y., Hoo, C. L., Myan, Y., & Wong, F. (2018). *Stabilising an Inverted Pendulum with PID Controller*. *02009*, 1–14.

Lundberg, K. H., Olin, F. W., & Barton, T. W. (1986). *History of Inverted-Pendulum Systems*.

Mansoor, H., & Bhutta, H. A. (2016). *Genetic Algorithm Based Optimal Back Stepping Controller Design For Stabilizing Inverted Pendulum*. *1*, 16–19.

Muškinja, N., & Tovornik, B. (2006). Swinging up and stabilization of a real inverted pendulum. *IEEE Transactions on Industrial Electronics*, *53*(2), 631–639. https://doi.org/10.1109/TIE.2006.870667

Nonlinear Control of the Inverted Pendulum on a Cart.pdf. (n.d.).

Olfati-saber, R. (2002). *@ L @ L*. *47*(2), 305–308.

Ozbek, N. S., & Efe, M. O. (n.d.). *Swing up and Stabilization Control Experiments for a Rotary Inverted Pendulum- An Educational Comparison*. 2226–2231.

Park, M. S., & Chwa, D. (2009). Swing-up and stabilization control of inverted-pendulum systems via coupled sliding-mode control method. *IEEE Transactions on Industrial Electronics*, *56*(9), 3541–3555. https://doi.org/10.1109/TIE.2009.2012452

Patra, A. K., Biswal, S. S., & Rout, P. K. (2019). Backstepping Linear Quadratic Gaussian

Controller Design for Balancing an Inverted Pendulum Backstepping Linear Quadratic Gaussian Controller Design for Balancing an. *IETE Journal of Research*, *0*(0), 1–15. https://doi.org/10.1080/03772063.2019.1592716

Shima, T. J., & Bashir, H. A. (2021). *PSO-Based Integral Sliding Mode Controller for Optimal Swing-Up and Stabilization of the Cart-Inverted Pendulum System*. *18*(2), 88–97.

Singh, J. (n.d.). *(Model-Based Control Design for Swing-up & Balance the Inverted Pendulum) Energy-Based Collocated Partial Feedback Linearization Control for Swing up LQR Control for Balance Submitted by*. 1–21.

Son, N. N., Pham, H. O., & Anh, H. U. Y. (2014). *HYBRID PD AND ADAPTIVE BACKSTEPPING CONTROL FOR SELF-BALANCING TWO-WHEEL ELECTRIC SCOOTER*. *4*, 347–360.

Tai, V. M., Tam, N. M., Do, T. V., Thien, T. D., Nguyet, N. T. M., Van Thuyen, N., & Hai, N. V. D. (2020). Back-stepping control for a rotary inverted pendulum. *Journal of Technical Education Science*, *59*(59), 93–101.

Wang, H. (2011). *Research on the key problems in the controller design for inverted pendulum system*. *2*, 2–5. https://doi.org/10.1109/ICICTA.2011.135

Wang, Y. (n.d.). *Masters' Thesis: Optimal Swing-Up Control of an Inverted Pendulum*.

Yusuf, L. A. (n.d.). *GA-PID Controller for Position Control of Inverted Pendulum*.

Appendix

MATLAB CODE

#matlab codes for backstepping state feedback controller

```
function SimBS_SF_SP
global M m g L
M= 0.94; m= 0.23; g= 9.81; L= 0.3302;
k1= -11.4164; k2= -10.5235; k3= 4.4350; k4= 21.8965; % tuned by GA with w= 0.1
t= 0; h= 0.01; loop= 1000;
x= [-1;0;pi/4;0]; yr= 1; % scenario 1
% x= [-1;0;-pi/4;0]; yr= 1; % scenario 2
% x= [1;0;-pi/4;0]; yr= -1; % scenario 3
% x= [1;0;pi/4;0]; yr= -1; % scenario 4

buf= [t x' 0];

for i= 1:loop
   sx3= sin(x(3));
   cx3= cos(x(3));
   E= 4/3*(M+m)-m*cx3^2;
   z= x(4)+k3*x(3);
   u1= L*E*(x(3)+k4*z+k3*(z-k3*x(3)));
   u2= (M+m)*g*sx3-m*L*(z-k3*x(3))^2*sx3*cx3;
   u= (u1+u2)/cx3-k1*(x(1)-yr)-k2*x(2);
   x= RK4(@fun,t,x,u,h);
   t= t+h;
   buf= [buf; t x' u];
end

subplot 311
plot(buf(:,1),buf(:,2),'k','linewidth',2)
%axis([0 10 -0.2 1.5])
xlabel('t(sec)'), ylabel('x_1(t)')
grid on
```

```
subplot 312
plot(buf(:,1),buf(:,4),'k','linewidth',2)
%axis([0 10 -0.05 0.2])
xlabel('t(sec)'), ylabel('x_3(t)')
grid on
subplot 313
plot(buf(:,1),buf(:,6),'k','linewidth',2)
%axis([0 10 -4 3])
xlabel('t(sec)'), ylabel('u(t)')
grid on

save 'BS_SP_SN1' 'buf'
%save 'BS_SP_SN2' 'buf'
%save 'BS_SP_SN3' 'buf'
%save 'BS_SP_SN4' 'buf'

function xdot= fun(t,x,u)
global M m g L
xdot= zeros(4,1);
sx3= sin(x(3));
cx3= cos(x(3));
E= 4/3*(M+m)-m*cx3^2;
xdot(1)= x(2);
xdot(2)= (-m*g*sx3*cx3+4/3*m*L*x(4)^2*sx3+4/3*u)/E;
xdot(3)= x(4);
xdot(4)= ((M+m)*g*sx3-m*L*x(4)^2*sx3*cx3-cx3*u)/(L*E);
```

#matab codes for lqr controller

```
function Sim_LQR_SP
global M m g L
M= 0.94; m= 0.23; g= 9.81; L= 0.33;
t= 0; h= 0.01; loop= 1000;
% x= [-1;0;pi/4;0]; yr= 1; % scenario 1
```

```
% x= [-1;0;-pi/4;0]; yr= 1; % scenario 2
%x= [1;0;-pi/4;0]; yr= -1; % scenario 3
x= [1;0;pi/4;0]; yr= -1; % scenario 4

A= [0 1 0 0;0 0 -3*m*g/(4*M+m) 0;0 0 0 1;...
    0 0 3*(M+m)*g/L/(4*M+m) 0];
B= [0; 4/(4*M+m);0;-3/L/(4*M+m)];
Q= diag([5 1 3 1]);  % Q= diag(5,1,3,1)
R= 0.1;                  % R= 1
K= lqr(A,B,Q,R);
k1= K(1); k2= K(2); k3= K(3); k4= K(4);

buf= [t x' 0];
K
for i= 1:loop
    u= -k1*(x(1)-yr)-k2*x(2)-k3*x(3)-k4*x(4);
    x= RK4(@fun,t,x,u,h);
    t= t+h;
    buf= [buf; t x' u];
end

subplot 311
plot(buf(:,1),buf(:,2),'k','linewidth',2)
%axis([0 10 -0.2 1.5])
xlabel('t(sec)'), ylabel('x_1(t)')

subplot 312
plot(buf(:,1),buf(:,4),'k','linewidth',2)
%axis([0 10 -0.15 0.2])
xlabel('t(sec)'), ylabel('x_3(t)')

subplot 313
plot(buf(:,1),buf(:,6),'k','linewidth',2)
%axis([0 10 -4 3])
```

```
xlabel('t(sec)'), ylabel('u(t)')

%save 'LQR_SP_SN1' 'buf'
%save 'LQR_SP_SN2' 'buf'
%save 'LQR_SP_SN3' 'buf'
%save 'LQR_SP_SN4' 'buf'
```

#matlab codes for load all programs in one to get in one figure

```
function DrawFig_MSP_SN1
clf
sz= get(0,'screensize');
set(gcf,'position',...
   [sz(3)/1.8 sz(4)/8 sz(3)/3 sz(3)/2.5]);

load 'BS_MSP_SN1';
t= buf(:,1); pBS= buf(:,2); aBS= rad2deg(buf(:,4)); uBS= buf(:,6);

load 'LQR_MSP_SN1';
pLQR= buf(:,2); aLQR= rad2deg(buf(:,4)); uLQR= buf(:,6);

subplot 311
h= plot(t,pBS,'g',t,pLQR,'r','LineWidth',1);
set(h(1),'LineWidth',2)
set(gca,'FontName','Arial','FontSize',11);
set(gca,'XLim',[0 40]);
set(gca,'XTick',[0 10 20 30 40],'XTickLabel',[0 10 20 30 40]);
set(gca,'YLim',[-2.5 2.5]);
set(gca,'YTick',[-2 -1 0 1 2],'YTickLabel',[-2 -1 0 1 2]);
xlabel('                    (a)                    t(sec)');ylabel('Position(m)');
legend('BSF','LQR','Location','NorthEast');
grid on
subplot 312
h= plot(t,aBS,'g',t,aLQR,'r','LineWidth',1);
```

```
set(h(1),'LineWidth',2)
set(gca,'FontName','Arial','FontSize',11);
set(gca,'XLim',[0 40]);
set(gca,'XTick',[0 10 20 30 40],'XTickLabel',[0 10 20 30 40]);
set(gca,'YLim',[-70 70]);
set(gca,'YTick',[-60 -30 0 30 60],'YTickLabel',[-60 -30 0 30 60]);
xlabel('                    (b)                    t(sec)');ylabel('Angle(deg)');
legend('BSF','LQR','Location','NorthEast');
grid on
subplot 313
h= plot(t,uBS,'g',t,uLQR,'r','LineWidth',1);
set(h(1),'LineWidth',2)
set(gca,'FontName','Arial','FontSize',11);
set(gca,'XLim',[0 40]);
set(gca,'XTick',[0 10 20 30 40],'XTickLabel',[0 10 20 30 40]);
set(gca,'YLim',[-100 150]);
set(gca,'YTick',[-100 0 100],'YTickLabel',[-100 0 100]);
xlabel('                    (c)                    t(sec)');ylabel('Control input');
legend('BSF','LQR','Location','NorthEast');
grid on
%% Performances
h= 0.01; yr= 1; y1= yr-pBS; y2= yr-pLQR;
e1= abs(yr-y1); e2= abs(yr-y2);
BS= stepinfo(y1,t,2*yr)
LQR= stepinfo(y2,t,2*yr)
IAE_BS= intg(e1,h);
IAE_LQR= intg(e2,h);
[IAE_BS, IAE_LQR]

function s= intg(x,h)
s= 0.5*h*(x(1)+2*sum(x(2:end-1))+x(end));
```

#matlab code for energy based passivity swing upenergy-basedh ba ckstepping state feed back controller

```
function feedbacksed passivity
energy-based
M=0.94;m=0.23;g=9.81;L=0.3302;
t=0;x=[0;0;pi;0];h=0.001;loop=10000;
 kv=5.723;kd=4;kx=13;ke=0.9;
% kv=1;kd=1;kx=0.02;ke=-1;
k1= -11.4164; k2= -10.5235; k3= 4.4350; k4= 21.8965;
% % D=rad2deg(x(3))
buf=[t x(1) x(3) 0 ];yr=0;
for i=1:loop
E=1/2*(m*L^2)*x(4)^2+m*g*L*(cos(x(3))-1);
p1=(kv*m*sin(x(3))*(L*x(4)^2-g*cos(x(3))))/M+m*sin(x(3))^2;
p2=kv/M+m*sin(x(3))^2;
num=-kx*x(1)-kd*x(2)+p1;
den=ke*E+p2;
u0=num/den;
sx3= sin(x(3));
    cx3= cos(x(3));
    E= 4/3*(M+m)-m*cx3^2;
    z= x(4)+k3*x(3);
    u1= L*E*(x(3)+k4*z+k3*(z-k3*x(3)));
    u2= (M+m)*g*sx3-m*L*(z-k3*x(3))^2*sx3*cx3;
    u3= (u1+u2)/cx3-k1*(x(1)-yr)-k2*x(2);
    u=u0+u3;

x= RK4(@fun,t,x,u,h);
t= t+h;
buf= [buf; t   x(1) x(3)   u ];

end
subplot 311
```

```
plot(buf(:,1),buf(:,2),'linewidth',2);
xlabel('t'),ylabel('x(1)'),legend('cart')
grid on
subplot 312
plot(buf(:,1),buf(:,3),'linewidth',2);
xlabel('t'),ylabel('x(3)'),legend('angle')
grid on
subplot 313
plot(buf(:,1),buf(:,3),'linewidth',2);
xlabel('t'),ylabel('u'),legend('control action')
grid on
```